svep1 and *tie1* genetically interact and affect aspects of facial lymphatic development in a Vegfc-independent manner

Melina Hußmann[1], Sarah Weischer[2], Claudia Carlantoni[3], Didier Y. R. Stainier[3], Thomas Zobel[4], Stefan Schulte-Merker[1]*

1 Institute of Cardiovascular Organogenesis and Regeneration, Faculty of Medicine, WWU Münster, Germany

2 Münster Imaging Network, Cells in Motion Interfaculty Centre, Department of Biology, WWU Münster, Germany

3 Max Planck Institute for Heart and Lung Research, Department of Developmental Genetics, Bad Nauheim, Germany

4 Münster Imaging Network, Cells in Motion Interfaculty Centre, WWU Münster, Germany

*Corresponding Author

Prof. Dr. Stefan Schulte-Merker

Institute for Cardiovascular Organogenesis and Regeneration

Mendelstraße 7

48149 Münster, Germany

email: schultes@ukmuenster.de

Abstract

Multiple factors are required to form functional lymphatic vessels. Here, we uncover an essential role for the secreted protein Svep1 and the transmembrane receptor Tie1 during the development of subpopulations of the zebrafish facial lymphatic network. This specific aspect of the facial network forms independently of Vegfc signalling, which otherwise is the most prominent signalling axis in all other lymphatic beds. Additionally, we find that multiple specific and newly uncovered phenotypic hallmarks of *svep1* mutants are also present in *tie1*, but not in *tie2* or *vegfc* mutants. These phenotypes are observed in the lymphatic vasculature of both head and trunk, as well as in the development of the dorsal longitudinal anastomotic vessel (DLAV) under reduced flow conditions. Furthermore, we show genetic interaction between *svep1* and *tie1* during the migration of parachordal lymphangioblasts (PLs). Therefore, our study demonstrates an important function for Tie1 signalling during lymphangiogenesis as well as blood vessel development in zebrafish and provides the first *in vivo* evidence for zebrafish Svep1 and Tie1 interaction. Since compound heterozygous mutations for *SVEP1* and *TIE2* have recently been reported in human glaucoma patients, our data have clinical relevance in demonstrating a role for Svep1 in Tie signalling in an in vivo setting.

Introduction

The lymphatic system is part of the vasculature and provides essential functions for tissue fluid homeostasis, absorption of dietary fats, and immune surveillance. Malfunction of the lymphatic vasculature can lead to severe lymphedema, obesity, or chronic inflammatory diseases (Mäkinen et al., 2021; Oliver et al., 2020). Since treatment options are rare and often only transiently effective, understanding the molecular mechanisms driving lymphangiogenesis is a prerequisite for the development of new therapeutic approaches (Mäkinen et al., 2021). To that end, mice and zebrafish have served as popular model organisms to study the development of lymphatic vessels and are commonly used for analyzing the underlying genetic and molecular mechanisms (Mäkinen et al., 2007; Padberg et al., 2017; van Impel and Schulte-Merker, 2014). Furthermore, many genes that are essential for lymphangiogenesis in zebrafish are evolutionarily conserved. Their inactivation leads to lymphatic defects in zebrafish and mice, and mutations in their orthologues are causative for

human diseases (Alders et al., 2009; Gordon et al., 2013; Hogan et al., 2009; Mauri et al., 2018; Wang et al., 2020). In the trunk vasculature of the zebrafish, so-called lympho-venous sprouts arise from the posterior cardinal vein at 32 hours post fertilization (hpf). They migrate dorsally and either remodel an intersegmental artery into a vein, or they migrate along the so called horizontal myoseptum (HM) as parachordal lymphangioblasts (PLs) at 2 days post fertilization (dpf). At 3 dpf, PLs migrate dorsally and ventrally to form the trunk lymphatic vasculature, consisting of the dorsal longitudinal lymphatic vessel, the intersegmental lymphatic vessels, and the thoracic duct (TD) (Hogan et al., 2009; Hogan and Schulte-Merker, 2017; Padberg et al., 2017). A separate lymphatic network, the facial lymphatics, arises in a distinctly different manner, originating from three progenitor populations: 1) the primary head sinus-lymphatic progenitors (PHS-LP), 2) a migratory angioblast cell near the ventral aorta, and 3) the major population sprouting from the common cardinal vein (CCV) (Eng et al., 2019). These progenitor populations proliferate, migrate and connect to each other in a relay-like mechanism (Eng et al., 2019). A third lymphatic bed is composed of the brain lymphatic endothelial cells (BLECs), which are single endothelial cells residing within the leptomeningeal layer of the zebrafish brain and that arise from the choroidal vascular plexus (Bower et al., 2017; van Lessen et al., 2017; Venero Galanternik et al., 2017). During larval stages, BLECs are often positioned next to meningeal blood vessels and stay at the distal periphery of the optic tectum and other brain regions (van Lessen et al., 2017). However, molecular mechanisms supporting the development of BLECs and facial lymphatics still need to be examined in more detail.

The best-studied pathway driving lymphangiogenesis comprises the growth factor vascular endothelial growth factor C (Vegfc), which is secreted as a pro-form that is processed through the concerted activity of Collagen and calcium-binding EGF domain-containing protein (Ccbe1) (Bos et al., 2011; Hogan et al., 2009; Jeltsch et al., 2014; Le Guen et al., 2014; Roukens et al., 2015) and a disintegrin and metalloproteinase with thrombospondin motifs (Adamts) 3/14 (Jeltsch et al., 2014; Wang et al., 2020) in the extracellular space. Fully processed VEGFC binds to its receptor VEGFR3 as well as VEGFR2 and induces lymphangiogenesis (Joukov et al., 1997; Karkkainen et al., 2004). Apart from the VEGFC/VEGFR3 pathway, TIE-ANG signalling was shown to be essential for lymphangiogenesis and vessel remodeling in mice and humans. This signalling cascade is composed of two receptor tyrosine kinases, tyrosine-protein kinase receptor 1 (TIE1) (Partanen et al., 1992) and tyrosine endothelial kinase (TEK), also known as tyrosine-protein kinase receptor 2 (TIE2) (Dumont et al., 1993), and multiple angiopoietin

ligands including angiopoietin 1 (ANG 1) (Davis et al., 1996; Suri et al., 1996) and angiopoietin 2 (ANG 2) (Maisonpierre et al., 1997). In mammals, TIE signalling is activated through binding of Angiopoietins to TIE2 (Davis et al., 1996; Maisonpierre et al., 1997). TIE1 can either block or activate the signalling cascade in a context dependent manner by forming heterodimers with TIE2 (Hansen et al., 2010; Marron et al., 2000; Saharinen et al., 2005; Savant et al., 2015; Seegar et al., 2010). *Tie1* knock-out mice display haemorrhages from E13.5 to P0, which lead to death and are preceded by lymphatic defects and edema formation from E12.5 onwards (D'Amico et al., 2010). In contrast to *Tie1* mutant mice, *Tie2* mutant mice die already at E9.5-10.5 due to defective cardiac development and vascular remodelling (Dumont et al., 1994; Sato et al., 1995). Conditional knockout of *Tie2* in lymphatic cells revealed the importance of TIE2 for lymphatic vessel development in mice especially for Schlemm's canal formation (Kim et al., 2017; Thomson et al., 2014). Recently, Korhonen et al. showed that conditional *Tie1* deletion, *Tie1;Tie2* double deletion and *Ang2* blocking resulted in impaired postnatal lymphatic capillary network development in mice (Korhonen et al., 2022). In zebrafish, *tie2* mutants do not have any vascular phenotypes (Gjini et al., 2011; Jiang et al., 2020), while *tie1* mutants show cardiac morphogenesis and vascular defects (Carlantoni et al., 2021).

In 2017, a new key player in lymphangiogenesis was discovered through genetic screens in zebrafish: *sushi, von Willebrand factor type A, EGF, and pentraxin domain-containing protein 1 (svep1)*, also referred to as *polydom* (Karpanen et al., 2017; Morooka et al., 2017). *svep1* encodes a large extracellular matrix molecule, with a total of 3555 amino acids and a variety of protein domains. The N terminal half of Svep1 mainly consists of complement control protein (CCP), also called sushi domain, repeats and EGF domains, indicating a possible role in protein binding stabilization. *Svep1-/-* mice show normal development of the primitive lymphatic plexus until E12.5, but then fail to form lymphatic valves and to undergo remodeling events of mesenteric lymphatic vessels at E18.5, accompanied by edema formation and death postnatally (Karpanen et al., 2017; Morooka et al., 2017). Recently, Michelini et al. reported possible implications of *SVEP1* in lymphedema formation in human patients, underlining the importance of SVEP1 for the lymphatic vasculature (Michelini et al., 2021). Additionally, SVEP1 is also required for Schlemm's canal formation in mice (Thomson et al., 2021). In zebrafish, *svep1* mutants exhibit a near-complete loss of the TD, demonstrating an essential function during lymphangiogenesis in zebrafish (Karpanen et al., 2017; Morooka et al., 2017).

In the present study, we show defects in the lymphatic head vasculature in *svep1* mutants, comprising a variable loss of BLECs and a specific facial lymphatic phenotype, which is complementary to the phenotypes observed in mutants of Vegfc/Vegfr3 pathway members. Therefore, we identified a lymphatic structure in the zebrafish that, in contrast to all other lymphatic structures, forms independently of the Vegfc/Vegfr3 pathway, but depends on Svep1.

However, until now, putative binding or interaction partners of Svep1 have not been confirmed *in vivo*. In this study, we first characterized novel lymphatic and blood vasculature phenotypes of *tie1* mutants, and subsequently realized that all phenotypic traits are shared between *tie1* and *svep1* mutants. These observations raised the question whether Svep1 and Tie1 interact, a notion that we tested genetically. Our results provide the first *in vivo* evidence for *svep1* and *tie1* genetic interaction, thus placing Svep1 as an important regulator of Tie1 function. Since recent clinical data suggested SVEP1 as a genetic modifier of TIE2-related Primary Congenital Glaucoma (PCG) (Young et al., 2020), our results have clinical relevance and will further help to understand the molecular basis of PCG.

Materials and Methods

Zebrafish strains

Animal work followed guidelines of the animal ethics committees at the University of Münster, Germany, and fish were maintained following FELASA guidelines (Aleström et al., 2020). The following transgenic and mutant lines have been used in this study: *Tg(flt4:mCitrine)*^{hu7135} (van Impel et al., 2014), *Tg(flt1*^{enh}*:tdTomato)*^{hu5333} (Bussmann and Schulte-Merker, 2011), *Tg(UAS:RFP)*^{nkuasrfp1a} (Asakawa et al., 2008), *Tg(vegfc:Gal4FF)*^{mu402} (Wang et al., 2020), *Tg(svep1:GAL4FF)*^{hu8885Tg} (Karpanen et al., 2017), *adamts3*^{hu10891}(Wang et al., 2020), *adamts14*^{hu11304} (Wang et al., 2020), *vegfc*^{hu6410} (Helker et al., 2013; Le Guen et al., 2014), *ccbe1*^{hu10965} (Kok et al., 2015), *svep1*^{hu6123} (Karpanen et al., 2017), *svep1*^{hu4767} (Karpanen et al., 2017) (only used for *svep1;ccbe1* double knockout, supplementary figure 2), *tie1*^{bns208} (Carlantoni et al., 2021), *tie2*^{hu1667} (Gjini et al., 2011), *Tg*^{BAC}*(apln:EGFP)*^{bns157} (Helker et al., 2020).

157 Genotyping

158 For genotyping of *svep1, adamts3, adamts14, vegfc and tie2* KASPar (Biosearch Technologies)
159 was used, and for *ccbe1* and *tie1* High-Resolution Melt Analysis (Samarut et al., 2016) (see
160 primer list table 1).
161
162 Live imaging and microscopy
163 Live imaging was carried out on 2 dpf, 3 dpf and 5 dpf embryos. Before 24 hpf, 1-Phenyl-2-
164 thiourea (PTU, 75 mM, Sigma, #P7629) was added to inhibit melanogenesis (Karlsson et al.,
165 2001). For imaging, embryos were anesthetized with 42 mg/L tricaine (Sigma, #A5040) and
166 embedded in 0.8 % low melting agarose (Thermo Fischer, #16520100) dissolved in embryo
167 medium. Embryo medium containing tricaine was layered on top of the agarose once solidified
168 for overnight imaging. Additionally, embryos were kept at 28 °C during overnight imaging.
169 Embryos were imaged with an inverted Leica SP8 microscope using a 20x/0.75 dry objective
170 or a 40x/1.1 water immersion objective detection and employing Leica LAS X 3.5.7.23225
171 software. Scoring of PLs or TD fragments was performed using a Leica M165 FC and an X-Cite
172 200DC (Lumen Dynamics) fluorescent light source. Confocal stacks were processed using Fiji-
173 ImageJ version 1.52g. Brightfield images were taken using an Olympus SZX16 microscope and
174 a LEICA DFC450 C camera. Images and figures were assembled using Adobe Illustrator. All data
175 were processed using raw images with brightness, color and contrast adjusted for printing.
176
177 Cell tracking
178 To quantify the migration distance and mean velocity of the PLs from 2.5 dpf to 3.5 dpf, the
179 leading edge of each PL was manually tracked using ,,Manual Tracking"-Plugin (Fabrice
180 Cordelières, Institut Curie, Orsay (France)) in Fiji-ImageJ (version 1.52g source (Schindelin et
181 al., 2012)). For image stabilization ,,StackReg" using rigid body (Thévenaz et al., 1998) was
182 applied to the maximum intensity projections of the timelapse movies prior to manual
183 tracking. Mean track velocity and total migration distance (sum of all leading edge
184 displacements) were calculated using a custom Python script (version 3.8). To plot the
185 migration route, track start coordinates were centered to the origin and individual cell tracks
186 were represented using a line plot (Python). Y PL migration was defined as the absolute value
187 of the distance in Y direction (dorsal and ventral) from track origin to the last tracking point
188 (ΔY). Scripts used for data analysis available at GitHub -

MuensterImagingNetwork/Hussmann_et_al_2022. Data was analyzed using GraphPad for plotting and statistical analysis.

Tricaine treatment

Embryos were treated with 0.014 % tricaine (Sigma, #A5040) from 30-48 hpf to slow down heart rate and blood flow during DLAV formation as previously described (Coxam et al. 2021).

In situ hybridization (ISH)

Antisense RNA probes of *tie1* were generated from amplified cDNA. Primers for cDNA generation are listed in supplementary table 1. Since the reverse primer contain a T3 overhang, we proceeded with in vitro transcription using T3 RNA polymerase and digoxigenin (DIG)-labeled UTP (2h at 37 °C). Fixation of 24 hpf embryos from a *svep1* heterozygous incrosses was performed with 4 % PFA overnight at 4 °C. ISH was performed according to previous published protocols using 100 ng of each of the respective probes (Schulte-Merker, 2002). Staining procedure was monitored until staining reached its maximum to ensure proper detection of differences in staining intensities between wildtype and mutant embryos.

Statistics and reproducibility

Data sets were tested for normality (Shapiro–Wilk) and equal variance p-values of data sets with normal distribution were determined by Welch's t-test or Student's t -test. In case data values did not show normal distribution, a Mann–Whitney test was performed instead. All statistical tests were performed using GraphPad Prism 8 or Microsoft Excel. All experiments were carried out at least two times. Only tricaine treatment of *vegfc* mutants (supplementary figure 5) was carried out once. However, no phenotype was observed in a large batch of embryos.

Results

Svep1 is required for FCLV formation in a Vegfc-independent manner

Since *svep1* mutants had previously been analyzed for lymphatic defects only in the trunk vasculature, we examined the head vasculature of *svep1* mutants to detect further possible malformations of the lymphatic system. At 5 dpf we observed that *svep1* mutants showed a

specific facial lymphatic phenotype, which seemed to be complementary to the facial lymphatic defects found in mutants of the Vegfc/Vegfr3 pathway members (Figure 1A). While mutants for Vegfc/Vegfr3 pathway members like *ccbe1*, *adamts3/14* and *vegfc* retained the facial collecting lymphatic vessel (FCLV) (red dotted line in Figure 1A, B) but lacked all other structures of the facial lymphatics, *svep1* mutants showed a specific loss of the FCLV. All other parts of the mature facial lymphatic network (including lymphatic branchial arches (LAA), lateral facial lymphatic (LFL), medial facial lymphatic (MFL) and otolithic lymphatic vessel (OLV) (blue dotted line in Figure 1A)) were only partially reduced in *svep1* mutants. Although the formation of the FCLV was strongly affected in all *svep1* mutants analyzed, the severity of the defects of facial lymphatic structures varied between individual *svep1* mutant embryos (supplementary figure 1). Only simultaneous interference of both the Vegfc and Svep1 signalling pathways completely blocked the development of all facial lymphatic structures (supplementary figure 2). To further characterize the differential roles of Svep1 and Vegfc during the formation of the facial lymphatic network, we examined the expression patterns of *svep1* and *vegfc* during sprouting of the PHS-LP, the progenitor cells of the FCLV, at 50 hpf using transgenic reporter lines. We detected *svep1* expression in cells juxtaposed to the sprouting LECs around the PHS, which later will form the FCLV, while *vegfc* expression was more restricted to the lateral facial lymphatic sprout arising from the CCV in all embryos analyzed (Figure 1C, supplementary figure 3). Taken together, these observations indicate a Vegfc-independent role of Svep1 during the development of distinct aspects of the facial lymphatics.

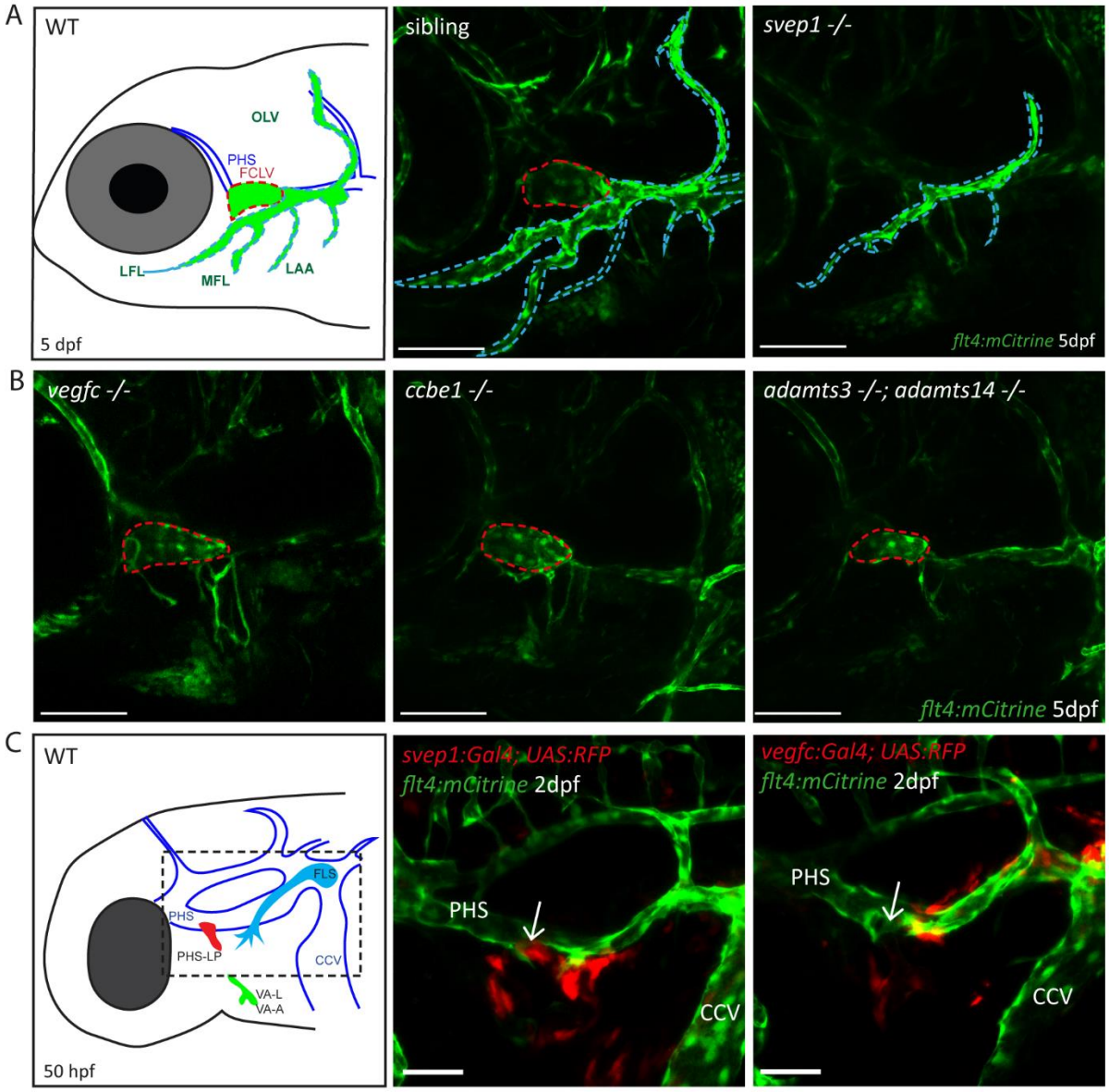

Figure 1: Svep1 is required for the development of the FCLV, in a Vegfc-independent manner.

A) Schematic representation of facial lymphatic network at 5 dpf and maximum intensity projection of confocal images of *flt4:mCitrine* positive *svep1* mutants (n=10) and siblings (n=6) highlighting facial lymphatic structures at 5 dpf. Scale bar= 100 µm. Note the absence of the FCLV (red dotted line) in *svep1* mutants whereas other facial lymphatic structures are less strongly affected (OLV, LFL, MFL, and LAA marked by blue dotted lines). B) Confocal images of *flt4:mCitrine* positive facial lymphatics in *vegfc* (n=19), *ccbe1* (n=5) and *adamts3*;*adamts14* (n=2) mutants at 5 dpf. Scale bar= 100 µm. C) Confocal images of *svep1* and *vegfc* expression domains during sprouting from the PHS at 2 dpf, with schematic representation of different lymphatic progenitor populations. *svep1* is expressed in close proximity to sprouting PHS-LPs, while *vegfc* expressing cells are more concentrated on the LECs arising from the CCV. Arrows point to sprouting PHS-LP. Scale bar= 50 µm. Expression patterns were confirmed in 6 embryos each (supplementary figure 3). CCV, common cardinal vein; FLS, facial lymphatic sprout; hpf, hours post-fertilisation; dpf, days post-fertilisation; LAA, lymphatic branchial arches; LFL, lateral facial lymphatic; MFL, medial facial lymphatic; OLV, otolithic lymphatic vessel; PHS, primary head sinus; PHS-LP, primary head sinus lymphatic progenitor; VA, ventral aorta; VA-L, ventral aorta lymphangioblast;

VA-A, ventral aorta angioblast; PHS, primary head sinus; FCLV, facial collecting lymphatic vessel; LEC, lymphatic endothelial cell; WT, wildtype.

Svep1 is essential for sprouting of BLECs and is expressed in close proximity to LECs

Since Svep1 is required for the formation of facial lymphatic structures (Figure 1), we wondered whether it is also involved in the development of an additional lymphatic vascular bed, the BLECs. In mutants of the Vegfc/Vegfr3 pathway, BLECs are completely absent (Bower et al., 2017; van Lessen et al., 2017). In *svep1* mutants, BLECs were found to be absent in most cases, but some embryos showed either reduced numbers or - in rare cases - even wildtype-like numbers of BLECs at 3 dpf (Figure 2A, B). In line with the idea that *svep1* is required for the sprouting and migration of BLECs, we observed *svep1* expressing cells in close proximity to the migrating BLECs at 3 dpf. (Figure 2C, D) Thus, there is close juxtaposition of *svep1* expressing cells with migrating LECs in all developing lymphatic structures examined, including the PLs in the trunk (Karpanen et al., 2017).

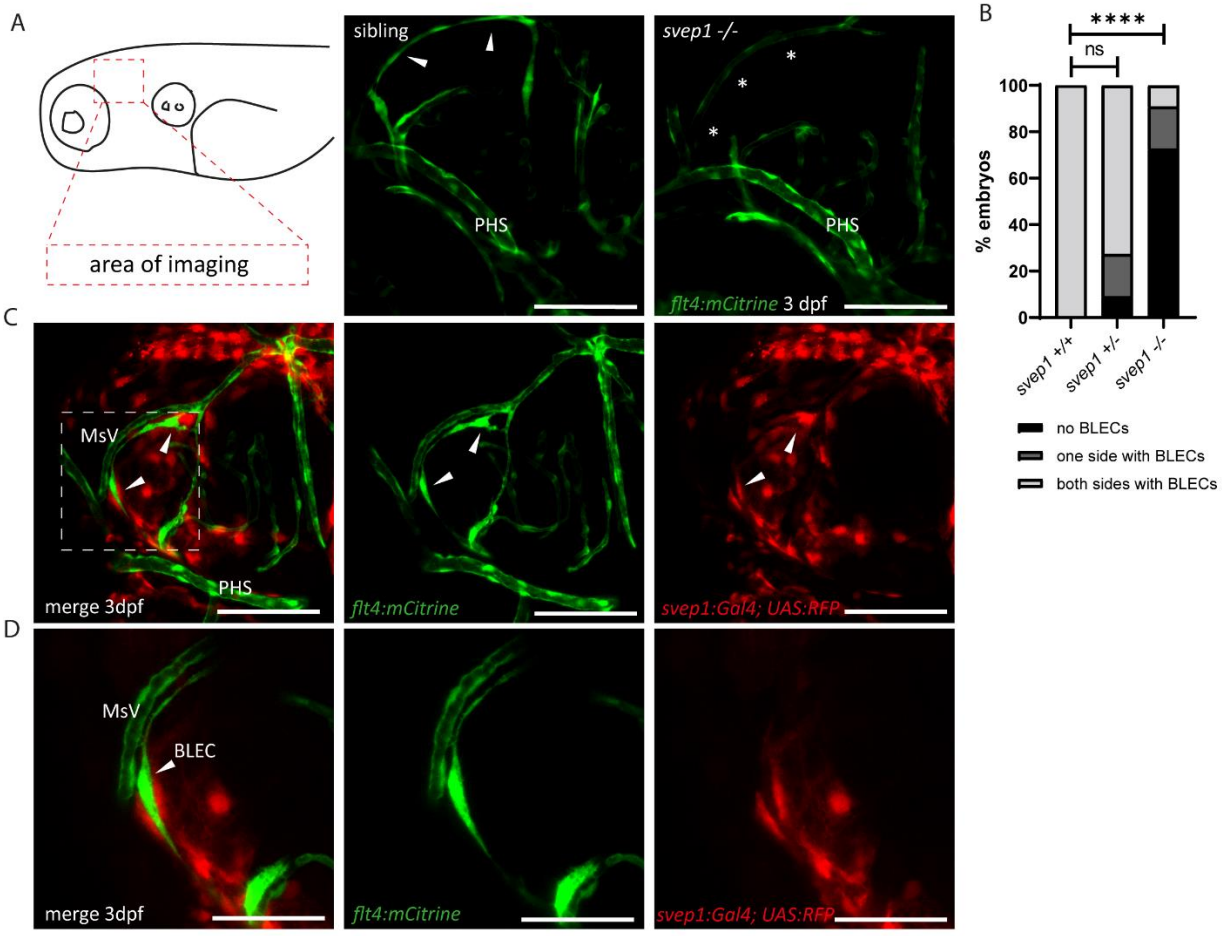

Figure 2: Svep1 is required for the sprouting of BLECs.

A) Confocal images of sprouting BLECs, marked by *flt4:mCitrine*, at 3 dpf in *svep1* mutants and siblings. Scale bar = 100 µm. B) Quantification of BLECs at 3 dpf on each side of the embryo showed that *svep1* mutants have significantly less BLECs on one or both sides of the brain hemispheres compared to siblings. For statistical analysis, no BLECs were counted as 0, BLECs being present on only one hemisphere as 1, whereas BLECs being detectable on both brain hemispheres were included as 2, for each embryo. (*svep1+/+*: n=10; *svep1+/-*: n=12; *svep1-/-*: n=12) Mann–Whitney test was applied for statistical analysis. Values are presented as means ± SD, ****P<0.0001, ns=not significant. Scale bar = 100 µm. C) Confocal images of *svep1:Gal4; UAS:RFP*, showing *svep1* expression immediately adjacent to BLECs, marked by arrows, at 3 dpf. Scale bar = 100 µm. D) Magnification and reduced stack numbers of boxed area in C). Arrow marks BLEC. Scale bar = 50 µm. PHS, primary head sinus; dpf, days post-fertilisation; BLEC, brain lymphatic endothelial cell; MsV, mesencephalic vein.

svep1 and *tie1* mutants show very similar lymphatic defects

SVEP1 has been shown to bind the TIE2 ligands ANG1 and ANG2 *in vitro*, regulate expression of *Tie1* as well as *Tie2* (Morooka et al., 2017), and has been suggested to play a role in *TIE2*-related primary congenital glaucoma (Young et al., 2020). Hence, we wanted to investigate the role of Tie signalling in zebrafish lymphangiogenesis in order to assess potential interactions with *svep1* in an *in vivo* situation. Trunk lymphatic phenotypes had not been previously reported in zebrafish mutants for either *tie1* or *tie2* (Carlantoni et al., 2021; Gjini et al., 2011; Jiang et al., 2020). Given the fact that there seems to be a very specific requirement for *svep1* for the development of the FCLV, we analysed facial lymphatic structures of *tie1* and *tie2* mutants in direct comparison to *svep1* mutants. Since *tie1* mutants developed strong edema at 4 dpf (data not shown), we focused our analysis on lymphatic phenotypes at 2 and 3 dpf to exclude secondary effects on the lymphatic vasculature. Significantly, *tie1* mutant embryos showed the same facial lymphatic defects as *svep1* mutant embryos at 3 dpf (Figure 3A), with the FCLV being strongly affected upon loss of *tie1*. This finding suggests that Tie1, either independently or in concert with Svep1 is responsible for FCLV formation in a Vegfc-independent manner. Examining other lymphatic cells, we found that *tie1* mutants did not show any BLECs at 3 dpf and exhibited significantly reduced numbers of PLs at 2 dpf, similar to *svep1* mutants (Figure 3B, C, D, E). Importantly, *tie2* mutant embryos, when examined for the same anatomical features, were found to display normal facial lymphatics, BLECs and PL numbers (Figure 3 A, B, C, E). Taken together, these findings demonstrate that loss of *tie1*, but not *tie2*, results in lymphatic phenotypes highly similar to the ones seen in *svep1* mutants, indicating that Svep1 constitutes an essential component acting in the Tie1 pathway.

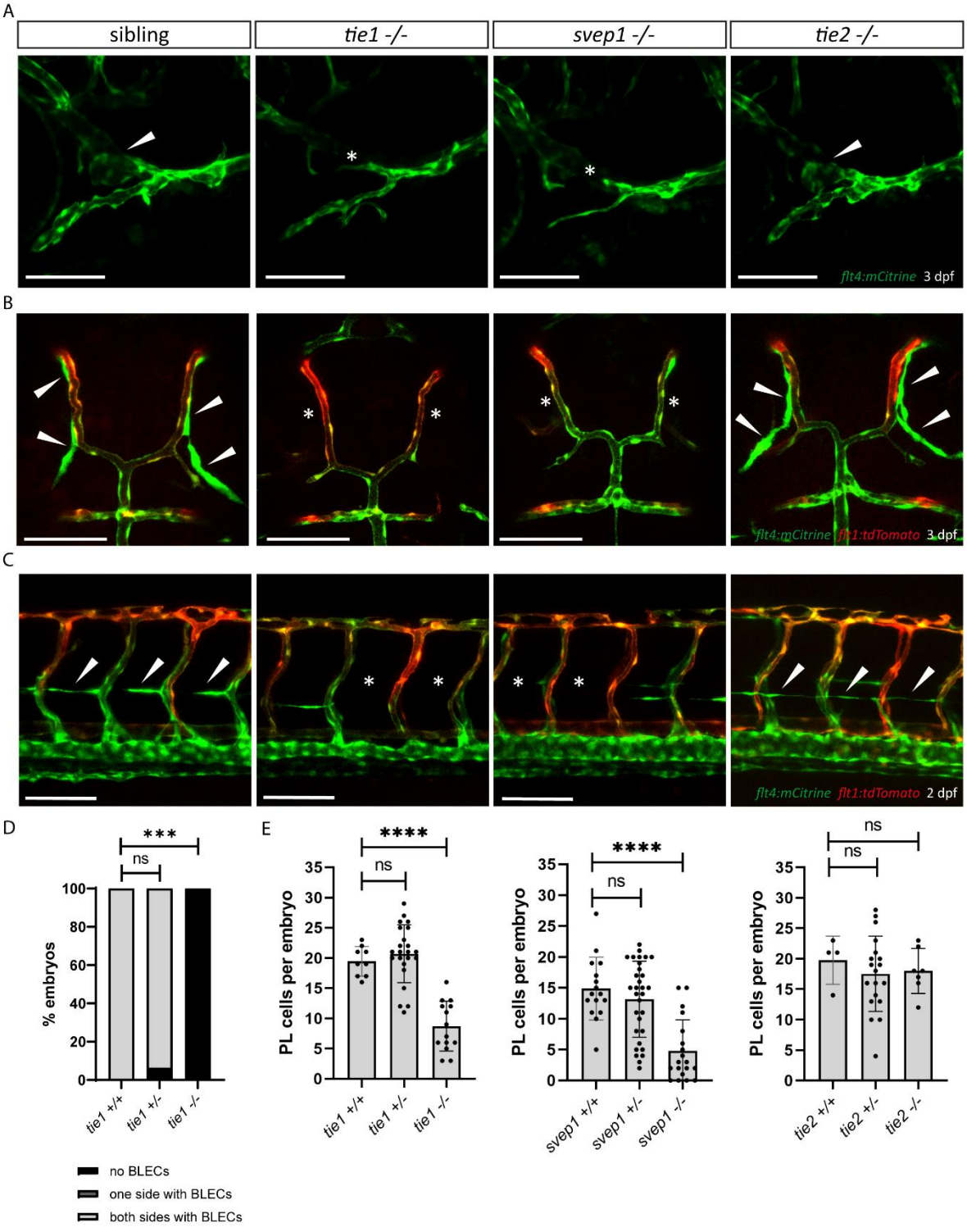

Figure 3: *tie1* mutants phenocopy the loss of *svep1*, while *tie2* is dispensable for lymphangiogenesis.

A) Facial lymphatics at 3 dpf in *flt4:mCitrine* positive *tie1*, *svep1* and *tie2* mutants and sibling embryos (lateral view). Arrows point to FCLV and asterisks indicate the absence of FCLV. Scale bar= 100 µm. B) *flt4:mCitrine; flt1:tdTomato* positive dorsal head vasculature in *tie1*, *svep1* and *tie2* mutants and in siblings at 3dpf (dorsal view). In *svep1* and *tie1* mutants (but not in *tie 2* mutants) the presence of BLECs is strongly reduced. Arrows point to BLECs and asterisks indicate areas lacking BLECs. Scale bar= 100 µm. C) Confocal images of PL cells, indicated by arrows, at 2 dpf in *flt4:mCitrine; flt1:tdTomato*

positive *tie1*, *svep1* and *tie2* mutants and siblings, showing reduced PL numbers in *svep1* and *tie1* mutants. Asterisks indicate missing PLs. Scale bar= 100 µm. D) Quantification of the presence of BLECs in *tie1* mutants compared to siblings. (*tie1+/+*: n=6; *tie1+/-*: n=16; *tie1-/-*: n=10) Mann–Whitney test was applied for statistical analysis. ***P=0.001, ns=not significant. E) Quantification of PL cell numbers in *tie1* (*tie1+/+*: n=9; *tie1+/-*: n=23; *tie1-/-*: n=14), *svep1* (*svep1+/+*: n=16; *svep1+/-*: n=31; *svep1-/-*: n=19) and *tie2* (*tie2+/+*: n=17; *tie2+/-*: n=27; *tie2-/-*: n=16) mutants compared to siblings. Mann–Whitney test was applied for statistical analysis. Values are presented as means ± SD, ****P<0.0001, ns=not significant; dpf, days post-fertilisation; PL, parachordal lymphangioblast; BLEC, brain lymphatic endothelial cell.

tie1 and *svep1* mutants display identical PL cell migration and survival defects

PLs first migrate along the HM and then start to migrate dorsally and ventrally along arteries to form the DLLV or the TD respectively. Previously, it was shown that PLs in *svep1* mutants fail to migrate dorsally or ventrally and rather remain at the HM (Karpanen et al., 2017). Here, we compared PL migration in *svep1* and *tie1* mutants using overnight imaging from 2.5 dpf to 3.5 dpf to analyse if PLs in *tie1* mutants phenocopy the PL migration defects of *svep1* mutants (Figure 4 A-L). While around 40-50% of PLs in sibling embryos migrated along the artery, only 11% of PLs in *tie1* and *svep1* mutants showed migration in either dorsal or ventral direction along the artery (Figure 4 M, N). Additionally, we observed around 33 % apoptotic PLs in *tie1* mutants and 55% in *svep1* mutants. These apoptotic events could be a consequence of failed migration, or could be due to decreased survival as a direct consequence of absent Svep1 or Tie1 activity. To further characterize migration of PLs in *svep1* and *tie1* mutants, we tracked and plotted the migration route of individual PLs (Figure 4 O, Q, Supplementary figure 4) and quantified the migration distance in the Y direction, (i.e. migration in dorsal or ventral direction), mean velocity and total migration distance in *tie1* and *svep1* mutants. PLs in *svep1* as well as in *tie1* mutants showed significantly less migration in ventral and dorsal directions compared to siblings, while the mean velocity and total migration distance were unchanged. Therefore, we can conclude that Svep1 and Tie1 are required for PL migration along the arteries in dorsal or ventral direction. Since we could observe the same specific migratory defects in both *svep1* and *tie1* mutants, these results further support a possible cross-talk between both proteins.

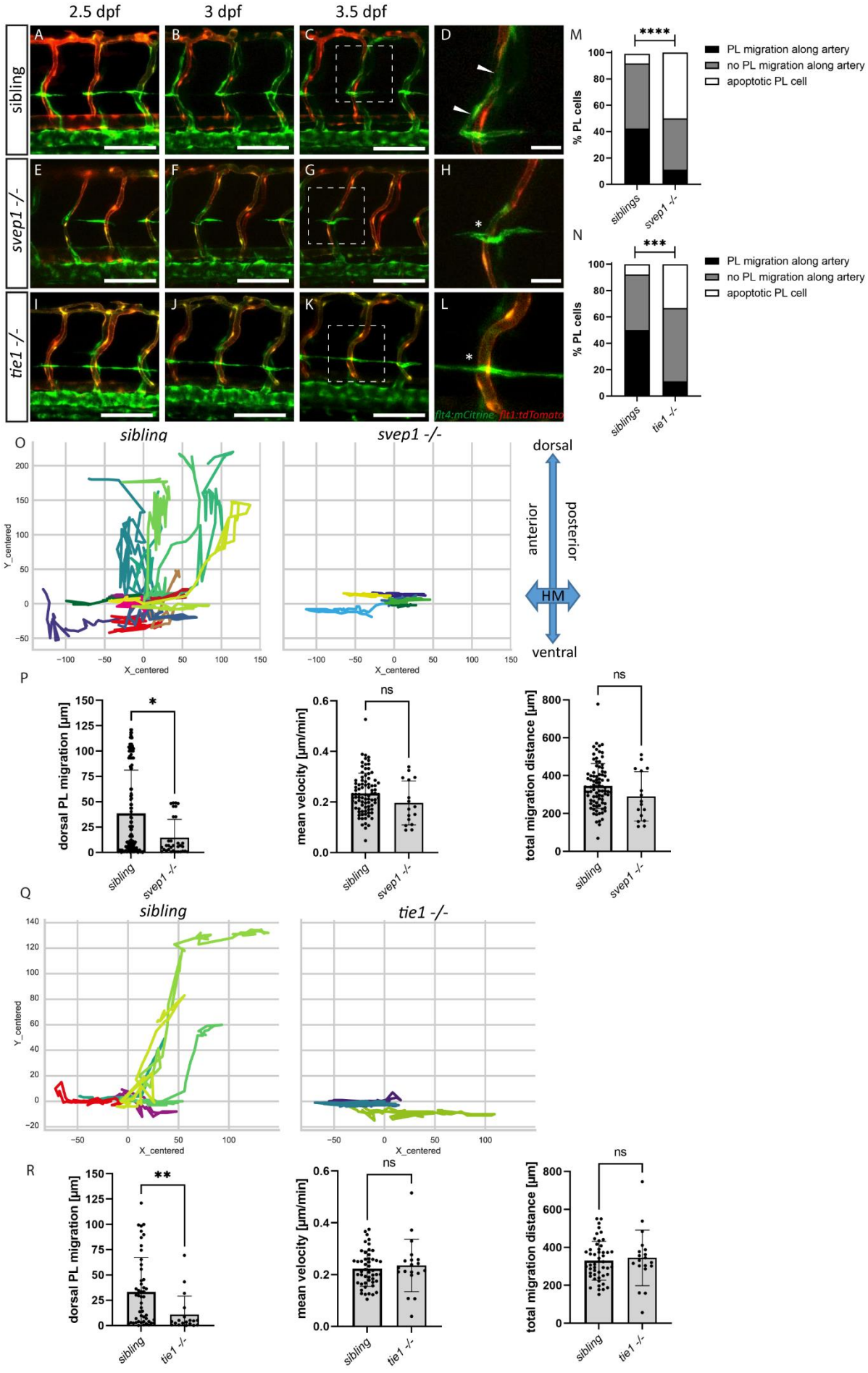

Figure 4: PL cell migration along arteries is severely affected in *svep1* and *tie1* mutants

A-L) Still frames from confocal time-lapse imaging of embryos in a *flt4:mCitrine; flt1:tdTomato* transgenic background. A-D) PL migration of sibling embryo along aISV (indicated by arrow) from 2,5 dpf to 3,5 dpf. E-F) failed PL migration (indicated by asterisk) of *svep1* mutants and I-L) *tie1* mutants along artery from 2,5 dpf to 3,5 dpf. M, N) Classification of PL migration along artery. Statistical analysis was performed using Mann–Whitney test comparing the % of PL migration along artery in each embryo between siblings and *mutants*. (*sibling*: n= 96 PLs in 18 embryos; *svep1-/-*: n= 36 PLs in 15 embryos; siblings: n=52 PLs in 14 embryos; *tie1-/-*: n=28 PLs in 10 embryos) ****P<0.0001 ***P=0.0003. O, Q) Representative cell tracking routes (tracks centered to origin) of single PL cells marked by different colours in siblings (n= 17 PLs in 4 embryos; n= 7 in 2 embryos), *tie1-/-* (n= 5 PLs in 2 embryos) and *svep1-/-* (n= 6 PLs in 3 embryos). P, R) Quantification of dorsal and ventral PL migration (delta Y migration distance), mean velocity and total migration distance in *svep1* and *tie1* mutants compared to sibling embryos (excluding apoptotic PLs quantified in M, N) revealed decreased migration in dorsal and ventral direction in *svep1* (*P=0.0148) as well as *tie1* mutants (**P=0.0023). ns= not significant; dpf, days post fertilization; PL, parachordal lymphangioblast; HM, horizontal myoseptum, aISV, arterial intersegmental vessel. Scale bar= 100µm (D, H, L=25 µm)

<u>*tie1* mutants show blood vascular defects under reduced flow conditions</u>

While *svep1* mutants were initially identified on the basis of their lymphatic phenotype (Karpanen et al., 2017), Coxam et al. recently showed that *svep1* mutant embryos display a unique vascular phenotype under reduced flow conditions (Coxam et al., 2022). Treatment of embryos with 0.014 % tricaine between 30 hpf and 48 hpf leads to incomplete formation of the dorsal longitudinal anastomotic vessel (DLAV) with gaps and unlumenised DLAV segments at 2 dpf in *svep1* mutant embryos. This phenotype is accompanied by increased Vegfa/Vegfr signalling and increased number of Apelin positive tip cells (Coxam et al., 2022). To investigate if *tie1* mutants mimic this very specific and unusual vascular defect, we treated embryos from *tie1* heterozygous parents with 0.014 % tricaine between 30 hpf and 48 hpf, and subsequently imaged the intersegmental vessels in the trunk. Our analysis showed that *tie1* mutants treated with tricaine exhibited significantly more gaps and fewer lumenised DLAV segments (Figure 5D) compared to both untreated *tie1* mutants (Figure 5B) and treated siblings (Figure 5 C, E, F), suggesting that Svep1 and Tie1 might interact not only in lymphangiogensis but also during blood vessel development. For *tie2* and *vegfc* mutants we did not observe any defects in DLAV formation upon tricaine treatment, indicating that this phenotype is specific for loss of Svep1 and Tie1 (supplementary figure 5). Additionally, upon tricaine treatment, and even in untreated conditions, *apelin* expressing ECs were increased in ISVs of *tie1* mutants as already shown for *svep1* morphants treated with tricaine in Coxam et al., 2022 (Figure 5 G-J). Since we observed increased apelin expressing ECs in *tie1* mutants already in untreated conditions we

388 investigated, if *svep1* morphants also show increased *apelin* expression even without tricaine
389 treatment (Figure 5 I, J). *svep1* morphants already showed increased apelin expression in the
390 ISVs in untreated conditions (supplementary figure 6). These observations indicate that *apelin*
391 is a downstream target of Tie1 as well as Svep1 even in untreated conditions and support the
392 hypothesis of Tie1 and Svep1 acting in the same molecular pathway.

393

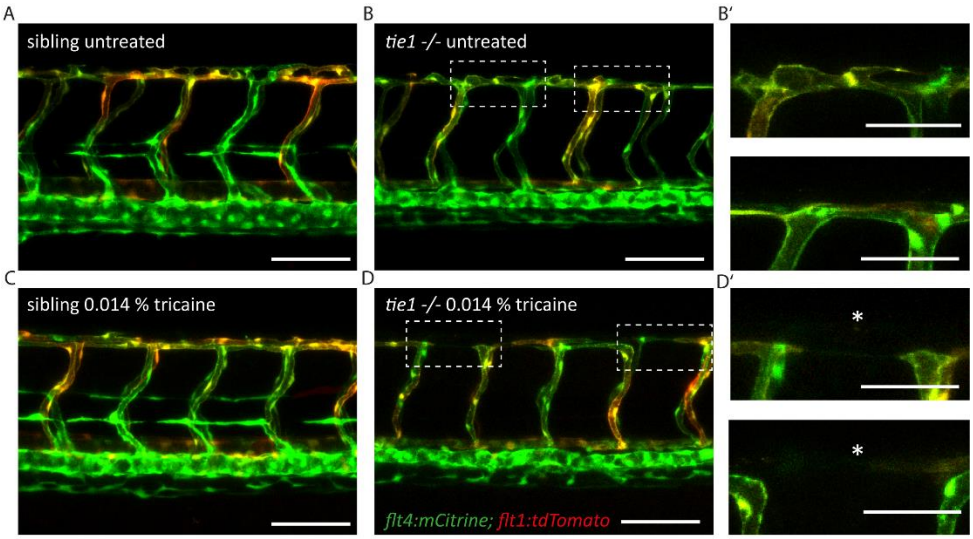

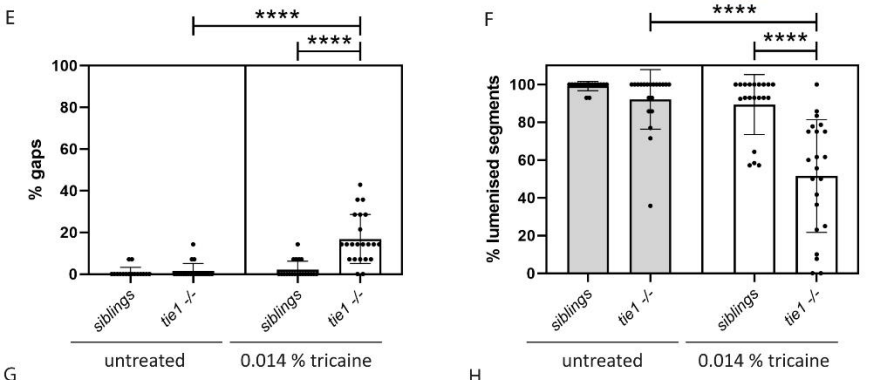

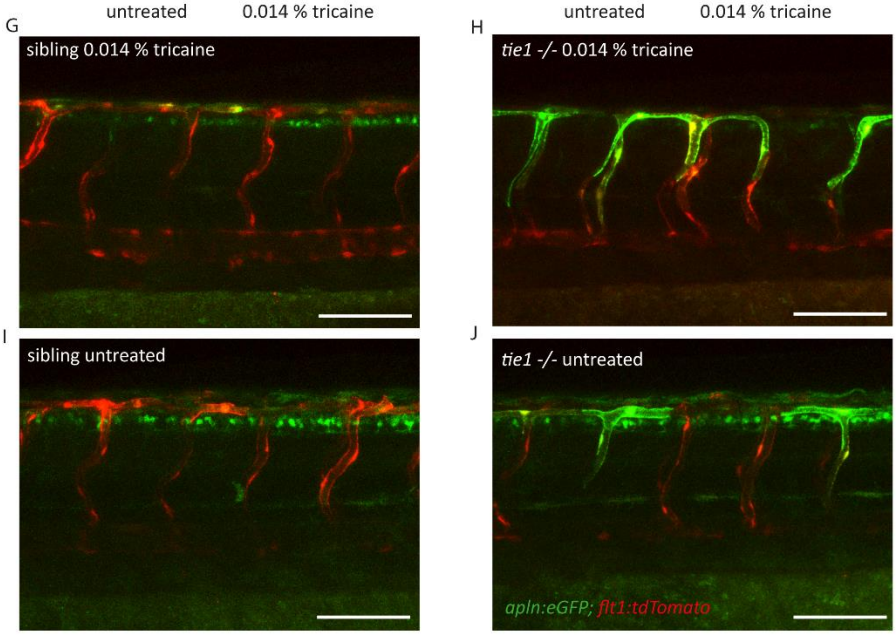

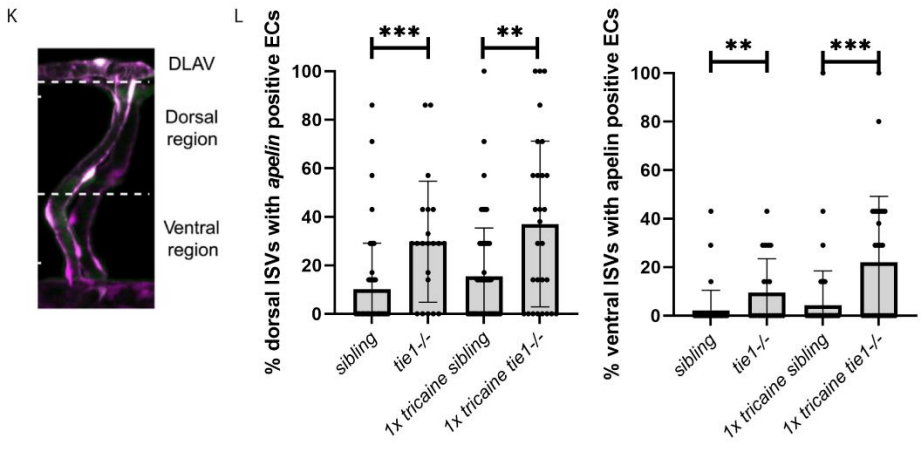

Figure 5: Reduced blood flow leads to vascular anastomosis defects in *tie1* mutants, similar to the defects in *svep1* mutants

A, B) Confocal images of sibling and *tie1* mutant embryos at 2 dpf in a *flt4:mCitrine* and *flt1:tdTomato* transgenic background. B') Magnification and reduced stack of boxed area in B). C, D) Confocal images of *sibling* and *tie1* mutant embryos treated with 0.014% tricaine from 30 hpf until 48 hpf. Asterisks indicate incompletely formed DLAV segments. D') Magnification and reduced stack numbers of boxed area in D). E) Quantification of gaps in the DLAV in sibling and *tie1* mutants that were either untreated or treated with 0.014 % tricaine revealed significant increase of gaps in the DLAV in *tie1* mutants according to Coxam et al., 2022. F) Quantification of lumenised trunk segments of the DLAV in siblings and *tie1* mutants, either untreated or treated with 0.014 % tricaine (siblings untreated: n= 16; *tie1-/-* untreated: n= 20; siblings treated with 0.014% tricaine: n= 20; *tie1-/-* treated with 0.014% tricaine: n= 22), revealed significant decrease of lumenised segments in the DLAV in *tie1* mutants. Mann–Whitney test was applied for statistical analysis. G, H) *apelin:eGFP* and *flt1:tdTomato* expression in 48 hpf old embryos after tricaine treatment from 30-48 hpf and I,J) in untreated conditions. K) Maximum intensity projection of an aISV at 48 hpf, highlighting the ventral and dorsal region used for further quantifications in J) adapted from (Coxam et al., 2022). L) Quantification of ISVs with apelin expression in dorsal and ventral parts of the ISVs. Dorsal part was counted from DLAV until midline region. Lateral region was counted from midline region onwards in ventral direction. *tie1* mutants showed significant increase of apelin positive ECs compared to siblings in untreated (dorsal: ***P=0.0001; ventral: **P=0.0028) and treated with 0.014 % tricaine conditions (dorsal: **P=0.0033; ventral: ***P=0.0002). (siblings untreated: n= 53; *tie1-/-* untreated: n= 21; siblings treated with 0.014% tricaine: n= 66; *tie1-/-* treated with 0.014% tricaine: n= 28). Mann–Whitney test was applied for statistical analysis. Values are presented as means ± SD. ****P<0.0001. Scale bar= 100 µm. hpf, hours post-fertilisation; dpf, days post-fertilisation; DLAV, dorsal longitudinal anastomotic vessel; ISV, intersegmental vessel.

<u>*tie2* loss of function does not exacerbate the *tie1* mutant phenotype</u>

To investigate a possible contribution of Tie2 to lymphatic Tie signalling as well as possible compensatory mechanisms, we examined *tie1; tie2* double mutants at 2 dpf (Figure 6 A-G). While *tie1* mutants showed a highly significant reduction in PL numbers (Figure 6 D, G), we found that an additional loss of one or two functional copies of *tie2* did not affect PL numbers in *tie1* mutant embryos (Figure 6 E, F, G). Additionally, loss of one *tie1* allele in *tie2* mutants did not result in any phenotype (Figure 6C, G). To further exclude contributions of Tie2 at later stages of lymphatic development on TD formation, we quantified the segments of TD across 10 consecutive trunk segments at 5dpf. In line with our analysis at 2 dpf, heterozygous loss of *tie1* did not reveal any phenotype in *tie2* mutants (Figure 6 H). These results therefore do not support a role of *tie2* in zebrafish lymphatic development.

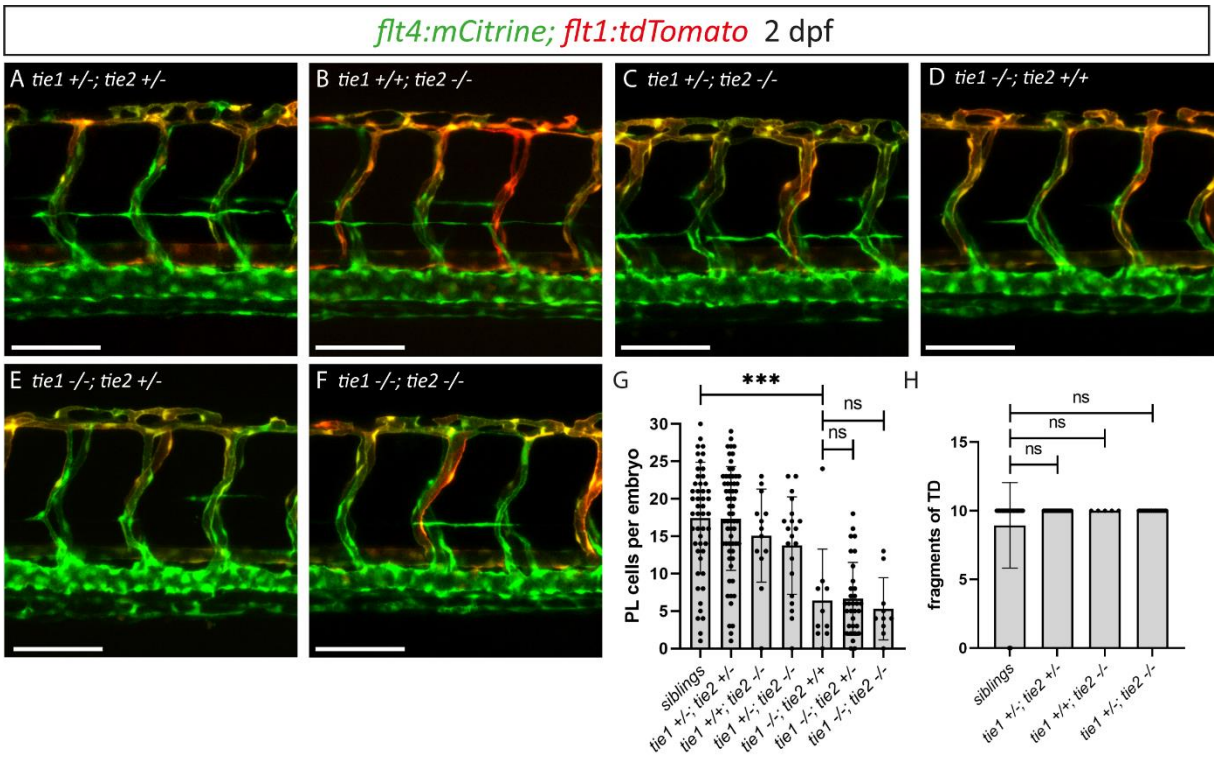

Figure 6: *tie1*; *tie2* double mutants show no exacerbation of the *tie1* mutant phenotype

A-F) Confocal images of blood and lymphatic vasculature in the trunk of 2 dpf old embryos derived from *tie1*; *tie2* double heterozygous fish, showing no genetic interaction between *tie1* and *tie2*. G) Quantification of PLs at 2 dpf and of thoracic duct fragments at 5 dpf (siblings: n=50; *tie1 +/-; tie2 +/-*: n=62; *tie1 +/+; tie2 -/-*: n=13; *tie1 +/-; tie2 -/-*: n=20; *tie1 -/-; tie2 +/+*: n=10; *tie1 -/-; tie2 +/-*: n=32; *tie1 -/-; tie2 -/-*: n=10). H) TD fragments were counted over the anterior-most 10 somites (siblings: n=47; *tie1 +/-; tie2 +/-*: n=34; *tie1 +/+; tie2 -/-*: n=5; *tie1 +/-; tie2 -/-*: n=16). Mann–Whitney test was applied for statistical analysis. ***P=0.0002, ns=not significant. Scale bar= 100 µm. dpf, days post-fertilisation; PL, parachordal lymphangioblast; TD, thoracic duct.

Genetic interaction between *svep1* and *tie1* during PL migration in the trunk

After having excluded a potential role for Tie2 during lymphangiogenesis, and given the high phenotypic similarity between *tie1* and *svep1* mutants, we wondered whether both genes might act in the same pathway during lymphangiogenesis and would therefore show a genetic interaction. To this end, we quantified PL cell numbers in embryos from *svep1; tie1* double heterozygous parents at 2 dpf. In *svep1; tie1* double heterozygous embryos we could not observe any PL number reduction compared to siblings (Figure 7 A, B, H), while *tie1* and *svep1* single mutants again showed severe reduction of PL cell numbers (Figure 7 C, D, H). Importantly, these defects were significantly exacerbated in *svep1*$^{+/-}$*; tie1*$^{-/-}$ compared to *svep1*$^{+/+}$*; tie1*$^{-/-}$ mutant embryos (Figure 7 D, F, H). In *svep1*$^{-/-}$*, tie*$^{+/-}$ mutant embryos, we

observed a tendency of less PLs compared to *svep1* single mutants (Figure 7 C, E, H). However, this effect was not significant. Taken together, this interaction study strengthens the idea that Svep1 converges in the Tie1 pathway.

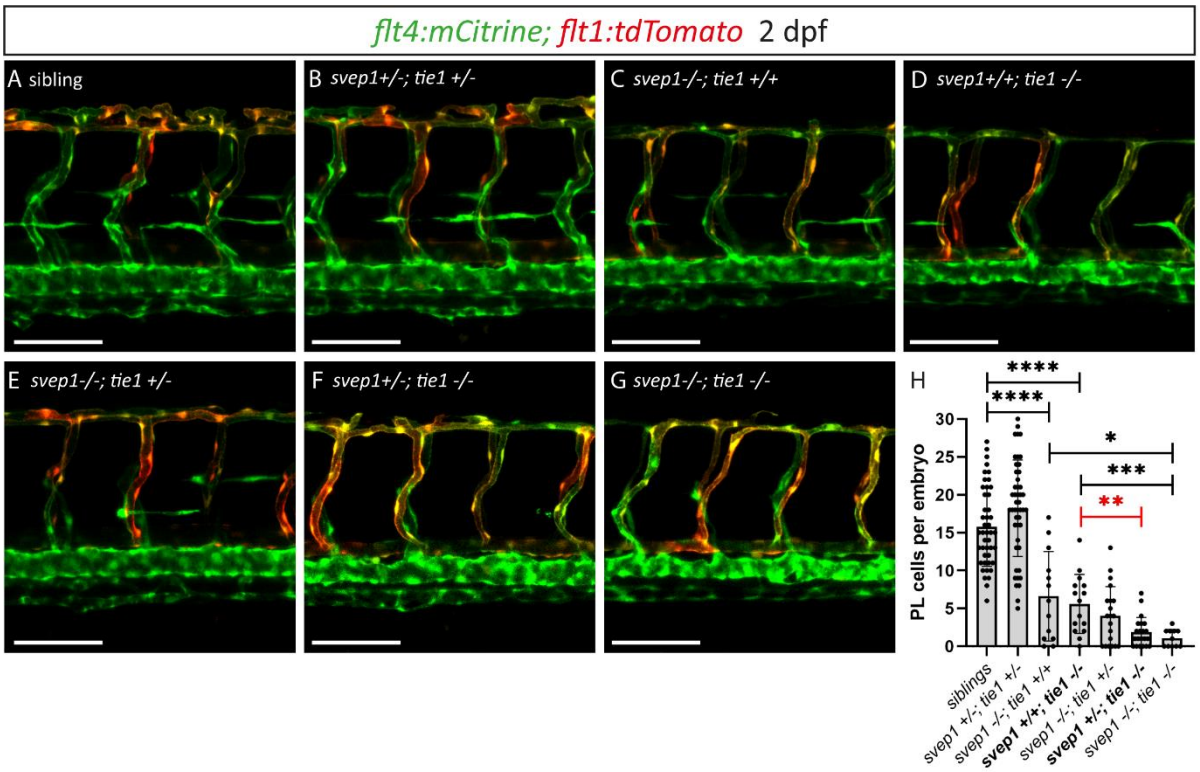

Figure 7: Heterozygous loss of *svep1* exacerbated the PL phenotype in *tie1* mutants, indicating genetic interaction between *svep1* and *tie1*

A-G) Confocal images of blood and lymphatic vasculature in the trunk of 2 dpf old embryos derived from *svep1; tie1* double heterozygous fish, showing severely reduced PL numbers in *svep1; tie1* double mutants and significant decrease of PL cell numbers in *svep1+/-; tie1-/-* compared to *svep1+/+; tie1-/-* (**P=0.0012). H) Quantification of PL cell numbers at 2 dpf using Mann–Whitney test (siblings: n= 45; *svep1 +/-; tie1 +/-*: n=45; *svep1 -/-; tie1 +/+*: n=13; *svep1 +/+; tie1 -/-*: n=15; *svep1 -/-; tie1 +/-* : n=20; *svep1 +/-; tie1 -/-*: n= 21; *svep1 -/-; tie1 -/-*: n= 11). Scale bar = 100 µm. Values are presented as means ± SD, ****P<0.0001, ***P=0.007, *P=0.0163, ns=not significant. dpf, days post-fertilisation; PL, parachordal lymphangioblast.

Discussion:

Svep1 is required for proper formation of functional lymphatic vessels. We here show an essential role for zebrafish Svep1 during formation of specific aspects of the facial lymphatic network and of BLECs. Additionally, we uncover a crucial role for Tie1 signalling during lymphangiogenesis and DLAV formation under reduced flow conditions in zebrafish and

provide strong *in vivo* evidence for *svep1* and *tie1* interaction. The results establish Svep1 as a factor in Tie1-signalling in zebrafish, both in lymphatic and vascular beds.

svep1 mutants display a very distinct phenotype in the facial lymphatic bed, which is complementary to the phenotypes we observed in mutants of Vegfc/Vegfr3 pathway members (Figure 1). Previous studies demonstrated that mutations in *vegfc*, *ccbe1* and *adamts3; adamts14* lead to a complete loss of the facial lymphatic vasculature, without assessing the effects on the recently described FCLV (Astin et al., 2014; Okuda et al., 2012; Padberg et al., 2017; Wang et al., 2020). In the present study, we show that the FCLV is still formed in mutants affecting the Vegfc/Vegfr3 signalling cascade, whereas mutations in either *svep1* or *tie1* result in a near-complete loss of this structure. In line with a differential requirement for *svep1/tie1* for the development of the facial lymphatic vessels and the facial collecting lymphatic vessel, we found that *svep1* is expressed in close proximity to the lymphatic sprout arising from the PHS giving rise to the FCLV while *vegfc* is expressed in cells that appear to be predominantly positioned around the migration route of the FLS arising from the CCV (Figure 1C). Based on this highly specific mutant phenotype, we conclude that Svep1 is essential for FCLV formation in a Vegfc-independent manner. Therefore, we here show for the first time that besides the previously postulated functional and morphological differences between FCLV and the facial lymphatics (Shin et al., 2019), there is also a difference in the pathways controlling the formation of both structures. Until recently, it was traditionally considered, that lymphatic vessels always 1) have a venous origin and 2) need Vegfc signalling to develop. In the last decade, it was shown that lymphatic vessels can also have non-venous origins in mice (Martinez-Corral et al., 2015) and also in the facial lymphatics of zebrafish (Eng et al., 2019). However, Vegfc signalling seemed to be always required for lymphatic vessel development. Interestingly, inactivation of *Angpt1* and *Angpt2* or *Tie2* completely abolishes Schlemm's Canal development and leads to glaucoma formation in mice, while the Schlemm's Canal is still present and only reduced in mice lacking *Vegfc* and *Vegfd* or *Vegfr3*, indicating that in some lymphatic structures VEGFC is not strictly required (Bernier-Latmani and Petrova, 2017; Thomson and Quaggin, 2018). Here we make the significant finding that a specific progenitor population of zebrafish facial lymphatic network, forming the FCLV, develops in a Vegfc independent and Svep1/Tie1 dependent mechanism. Since the Schlemm's canal is a hybrid vessel (Kizhatil et al., 2014) and the FCLV seem to be also morphological and functional

different from other lymphatic vessels (Shin et al., 2019), these two vessels not only share mechanistical but also functional differences to other lymphatic structures.

While the majority of mutants identified in forward genetic screens affect known or novel members of the Vegfc signalling pathway with highly similar phenotypes, the *svep1* mutants stand out due to phenotypic differences compared to mutants affecting the *Vegfc/Vegfr3* pathway. This, however, raises the question how Svep1 exerts its effects during lymphangiogenesis. In the current study we focused on a potential connection to the Tie signalling pathway, as murine ANG1 and ANG2 had been shown to bind Svep1 *in vitro* (Morooka et al., 2017). In mice, conditional knockout of *Svep1* or *Tie2* leads to high intraocular pressure and altered Schlemm's canal morphology (Li et al., 2020; Thomson et al., 2014). Additionally, *Tie2* and *Tie1* expression levels are downregulated in *Svep1* mutant mice (Morooka et al., 2017).

While *Tie2* knock-out mice display severe cardiovascular defects and die at E9.5 (Dumont et al., 1994; Sato et al., 1995), *tie2* mutant zebrafish show unaltered vascular structures including unaffected trunk lymphatics (Gjini et al., 2011; Jiang et al., 2020). We here extended that notion to lymphatic beds in the head of the embryo: as is the case for PL cell numbers, neither the formation of facial lymphatics nor of BLECs depend on Tie2 activity. Teleost *tie2* has actually been lost in the Acanthomorphata lineage, comprising 60% of contemporary teleost species (Jiang et al., 2020), suggesting either the loss of critical Tie2 function in most teleosts, or the adoption of essential functions for mammalian TEK function within the last 450 million years (dos Reis et al., 2015). This complicates functional comparison between mammalian and teleost Ang/Tie signalling. *Tie1* mutant mice do not show any vascular defects until E13.5 and die from haemorrhages between E13.5 and P0, but display swellings at E12.5 caused by lymphatic malformations that precede the haemorrhaging (D'Amico et al., 2010; Puri et al., 1995; Sato et al., 1995). Additionally, postnatal *Tie1* deletion causes impaired lymphatic capillary network development (Korhonen et al., 2022). We here show that *tie1* mutant zebrafish embryos display severe lymphatic defects in the head and trunk vasculature, in addition to the previously reported cardiac and blood vascular phenotypes including impaired brain angiogenesis, reduced CCV width, and impaired caudal vein plexus formation (Carlantoni et al., 2021). Interestingly, the FCLV, which seem to have a comparable function to collecting lymphatic vessels, is affected in *tie1* mutant zebrafish embryos, while *Tie1;Tie2* double

deletion in mice leads to defective postnatal collecting lymphatic vessel development (Korhonen et al., 2022). Further studies will be required in both mice and fish to determine to what extent Tie signalling affects LEC specification, proliferation, and survival. However, we here show definitively that Tie signalling is not only required in mice and humans for lymphatic vessel formation, but also in zebrafish.

Remarkably, lymphatic and non-lymphatic phenotypes observed in *tie1* mutant zebrafish embryos are very similar to the defects observed in *svep1* mutants: while reduced PL numbers and TD length is a hallmark feature of many lymphatic mutants, the specific absence of the FCLV is unique, and common to both mutants. Furthermore, formation of BLECs is affected in both mutants, and the specific PL migration phenotype, with PL cells at the horizontal myoseptum not migrating dorsally or ventrally, is also observed in both *svep1* and *tie1* mutants (Figure 4). In addition, we could show that *tie1* mutants show similar vascular defects in DLAV formation under reduced flow conditions compared to *svep1* mutants, while we did not observe any defects in *vegfc* and *tie2* mutants. Another hallmark of a *svep1* phenotype is the increase in *apelin* expression in the ISVs, which is again recapitulated in *tie1* mutants. Therefore, we conclude that *svep1/tie1* signalling is not only important for lymphangiogenesis but also for blood vessel development and acts to some extent in a Vegfc independent manner. Finally, genetic interaction studies indicate that Svep1 provides essential input into the Tie1 pathway, as losing one copy of *svep1* in *tie1* mutants exacerbates the phenotype significantly when assessing PL cell numbers (Figure 7). Of note, elimination of both *tie2* alleles did not alter the *tie1* mutant phenotype (Figure 6). Since Young et al. (2020) reported Svep1 as a genetic modifier of *TIE2* (Young et al., 2020), and Morooka et al. showed that *Tie1* as well as *Tie2* expression levels are downregulated in *Svep1* deficient mice (Morooka et al., 2017), we assessed *tie1* expression levels in zebrafish *svep1* mutants. However, using *in situ* hybridisation, we did not find any signs of misregulation of *tie1* expression in *svep1* mutants (supplementary figure 7), indicating that at least in zebrafish downregulation of *tie1* is not causative for the phenotype. Rather, and based on the observation that Svep1 can bind Tie receptor ligands (Morooka et al., 2017), we propose that Svep1 most likely stabilizes ligand-receptor binding. Due to the close proximity of *svep1* expressing cells to LECs and the fact that Svep1 is a large protein with several CCP domains, we suggest that Svep1 might act as a chaperon to help accumulation of Angiopoietins and induces Tie signalling in endothelial cells. Taken together, we provide the first *in vivo* evidence that Svep1 interacts with Tie1, and that

both genes, at least in certain vascular beds, act in a Vegfc-independent manner. Thus, we here clarify the importance of the respective roles of Tie1 as well as Tie2 in zebrafish, but also underline the significance of Svep1 and Tie signalling in vascular development. Together with the recent discovery that SVEP1 could act as a modifier of TEK-related PCG disease penetrance, further studies in zebrafish can serve as an *in vivo* model for clinically relevant aspects of Svep1/Tie signalling.

Acknowledgments:

This work was supported by CRC 1348 (DFG, project B08, M.H., S.S.M.) and by the CiM-IMPRS graduate school.

Competing interests:

none

Author contributions:

M.H. and S.S.M. conceptualized the project and wrote the manuscript. M.H. performed the experiments. S.W. and T.Z. provided infrastructure and codes for image analyses. C.C. and D.Y.R.S. provided the *tie1*^{bns208} zebrafish strain prior to publication. All authors commented on the manuscript.

Supplementary data:

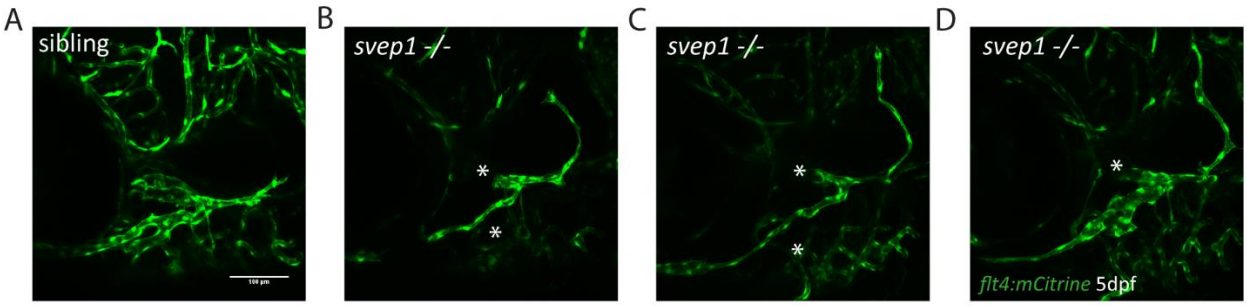

Supplementary figure 1: Facial lymphatic phenotype of *svep1* mutant embryos

A-D) Confocal images of siblings and *svep1* mutant embryos at 5dpf, expressing the *flt4:mCitrine* transgene. Asterix indicates reduced lymphatic vessels. Scale bar= 100 µm.

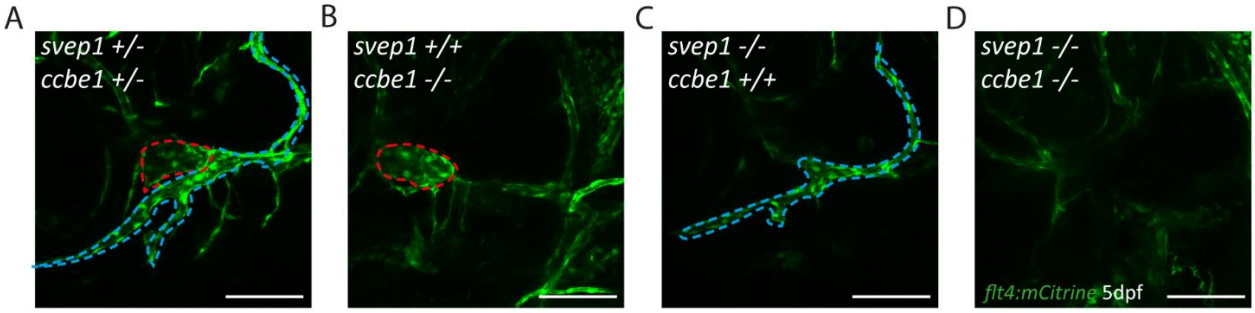

Supplementary figure 2: Combined loss of *svep1* and *ccbe1* leads to a loss of all facial lymphatic structures

A-D) Facial lymphatic phenotype of *svep1; ccbe1* double mutants (n=6) at 5dpf expressing *flt4:mCitrine*. OLV, LVL, MFL, marked by blue dotted lines. FCLV marked by red dotted lines. Scale bar= 100 µm. LFL, lateral facial lymphatic; MFL, medial facial lymphatic; OLV, otolithic lymphatic vessel; FCLV, facial collecting lymphatic vessel.

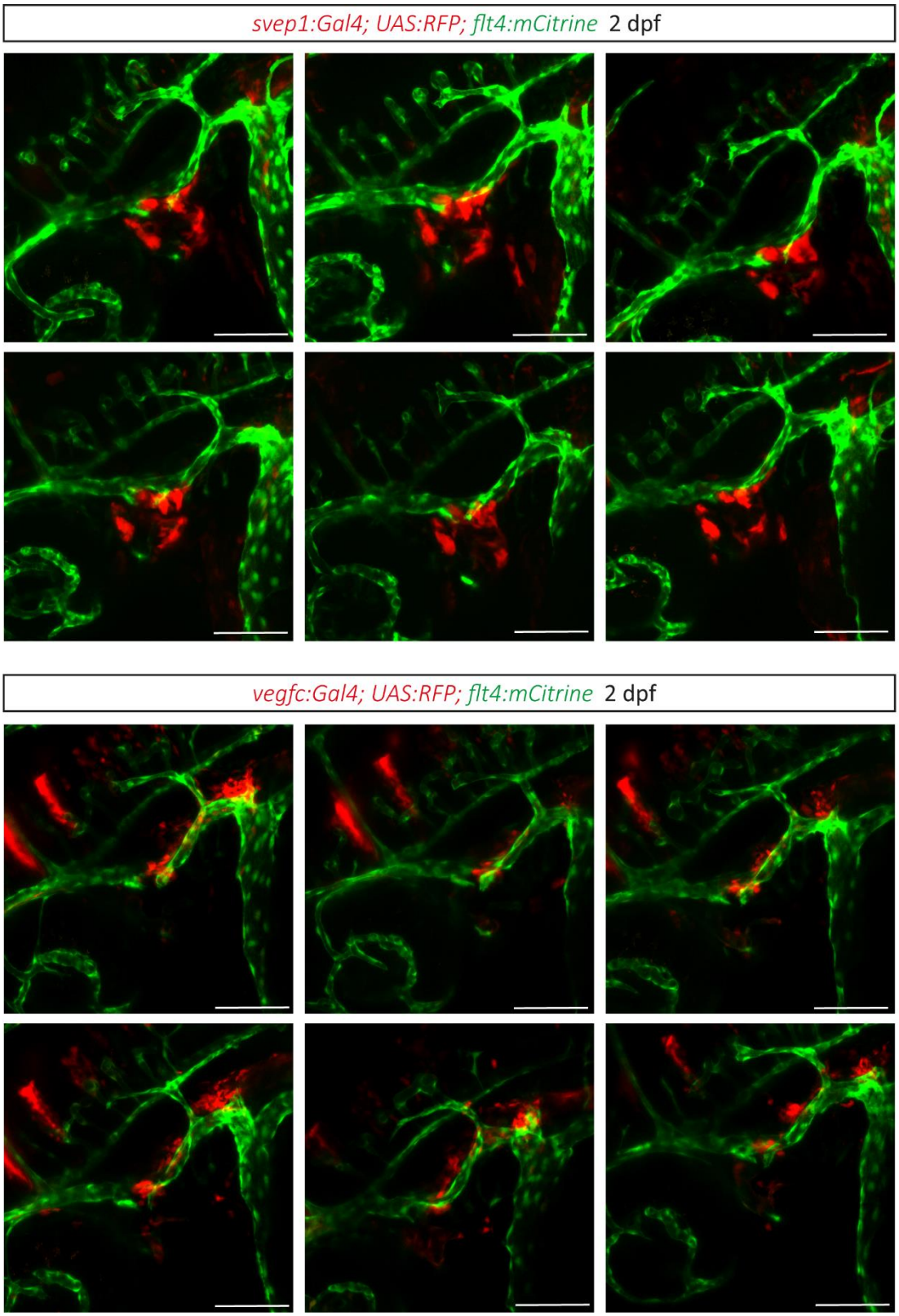

Supplementary figure 3: *svep1* and *vegfc* expression

Confocal images of *svep1:Gal4; UAS:RFP; flt4:mCitrine* and *vegfc:Gal4; UAS:RFP; flt4:mCitrine* transgenic embryos 2 dpf. Scale bar=100µm.

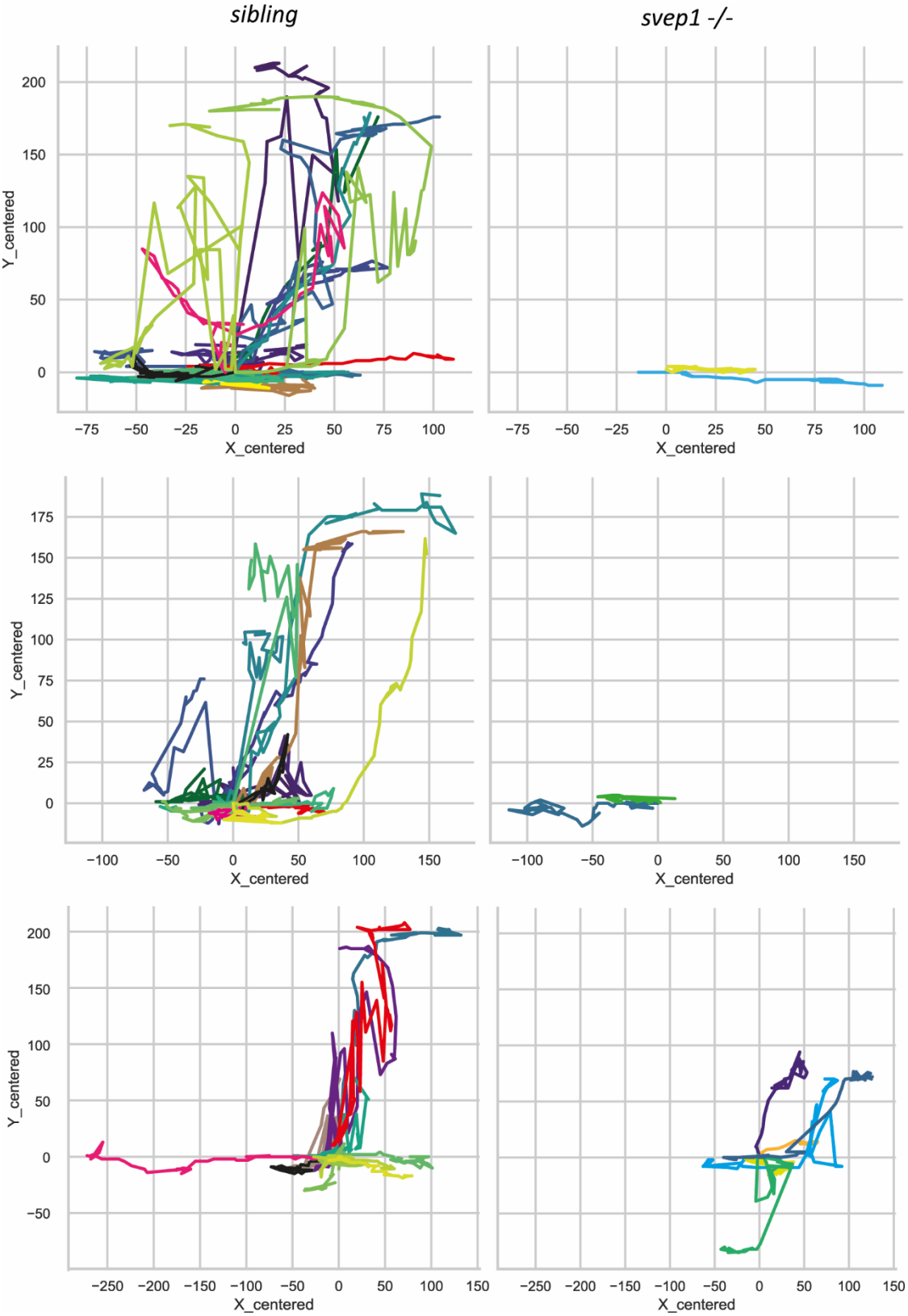

603

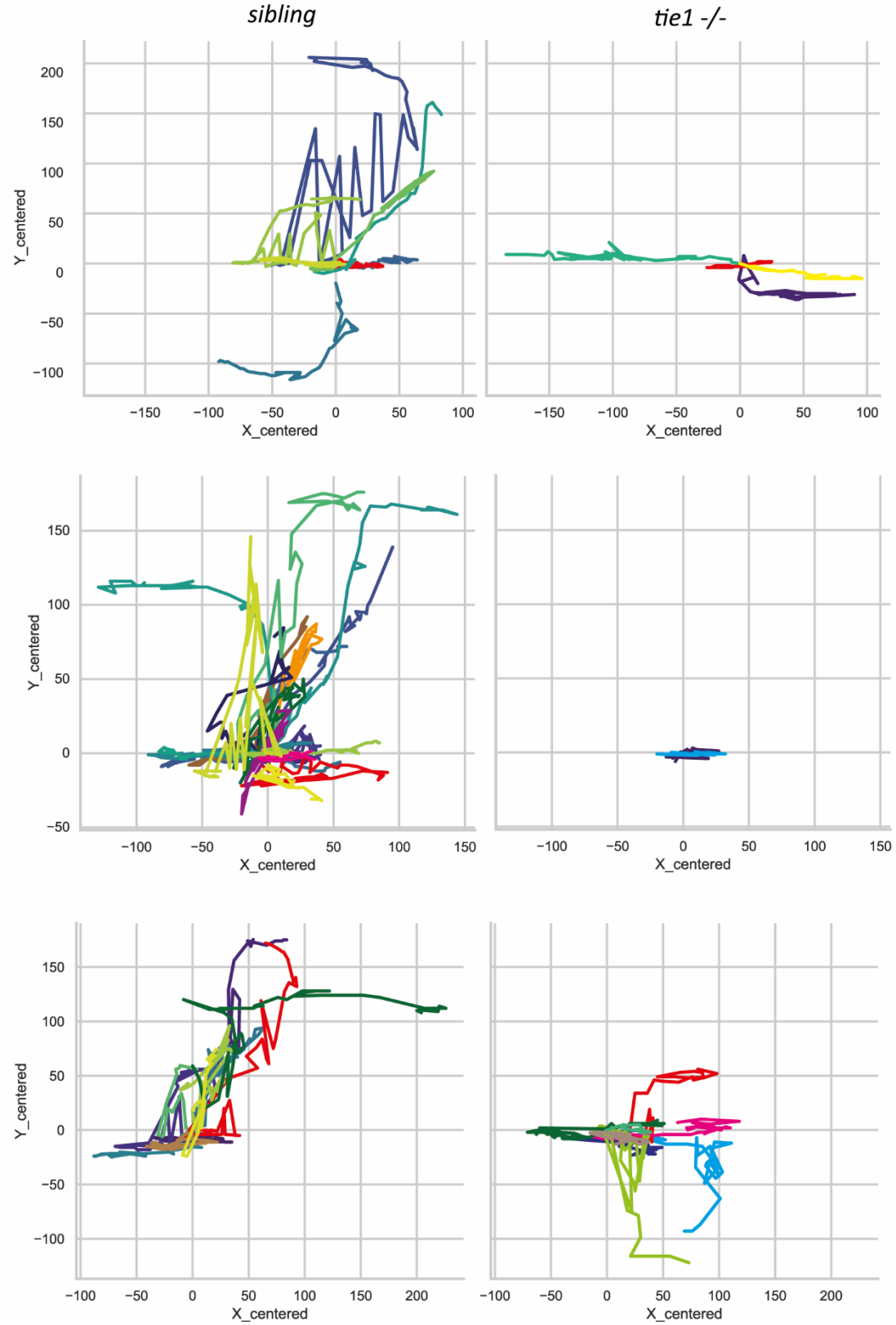

Supplementary figure 4: *svep1* and *tie1* mutants display PL migration defect

Additional cell tracking routes of PL cells in *svep1* (n= 12 PLs in 5 embryos) and *tie1* mutants (n=14 PLs in 6 embryos) from 2.5 dpf to 3.5 dpf compared to siblings (n=72 PLs in 14 embryos + 42 PLs in 12 embryos) tracked with manual tracking tool. dpf, days post fertilization; PL, parachordal lymphangioblast

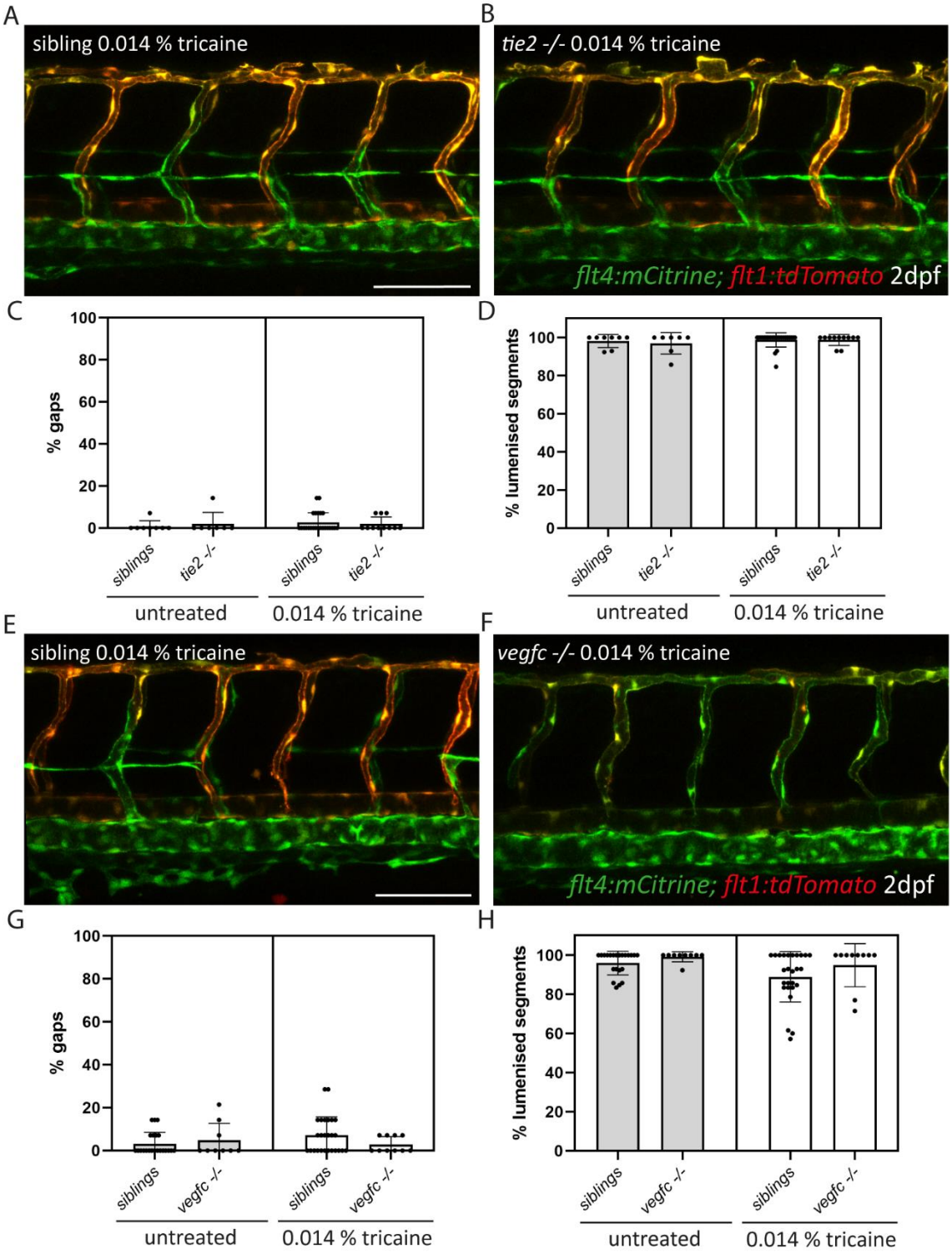

Supplementary figure 5: *vegfc* and *tie2* mutants do not show defects in DLAV formation upon tricaine treatment

A, B) Confocal images of *sibling* and *tie2* mutant embryos, expressing *flt4:mCitrine* and *flt1:tdTomato* at 2 dpf treated with 0.014 % tricaine from 30 hpf until 48 hpf. C) Quantification of gaps in the DLAV in sibling and *tie2* mutants that were either untreated or treated with 0.014 % tricaine (siblings untreated: n=8; *tie2-/-* untreated: n=7; siblings treated with 0.014 % tricaine: n= 24; *tie2-/-* treated with 0.014% tricaine: n= 11). D) Quantification of lumenised trunk segments of the DLAV in siblings

and *tie2* mutants, either untreated or treated with 0.014 % tricaine. E, F) Confocal images of *sibling* and *vegfc* mutant embryos, expressing *flt4:mCitrine* and *flt1:tdTomato* at 2 dpf treated with 0.014 % tricaine from 30 hpf until 48 hpf. G) Quantification of gaps in the DLAV in sibling and *tie2* mutants that were either untreated or treated with 0.014 % tricaine (siblings untreated: n=22; *vegfc-/-* untreated: n=9; siblings treated with 0.014 % tricaine: n= 26; *vegfc-/-* treated with 0.014 % tricaine: n= 10). H) Quantification of lumenised trunk segments of the DLAV in siblings and *tie2* mutants, either untreated or treated with 0.014 % tricaine. Mann–Whitney test was applied for statistical analysis. Scale bar= 100µm. dpf, days post-fertilisation; DLAV, dorsal longitudinal anastomotic vessel; ISV, intersegmental vessel

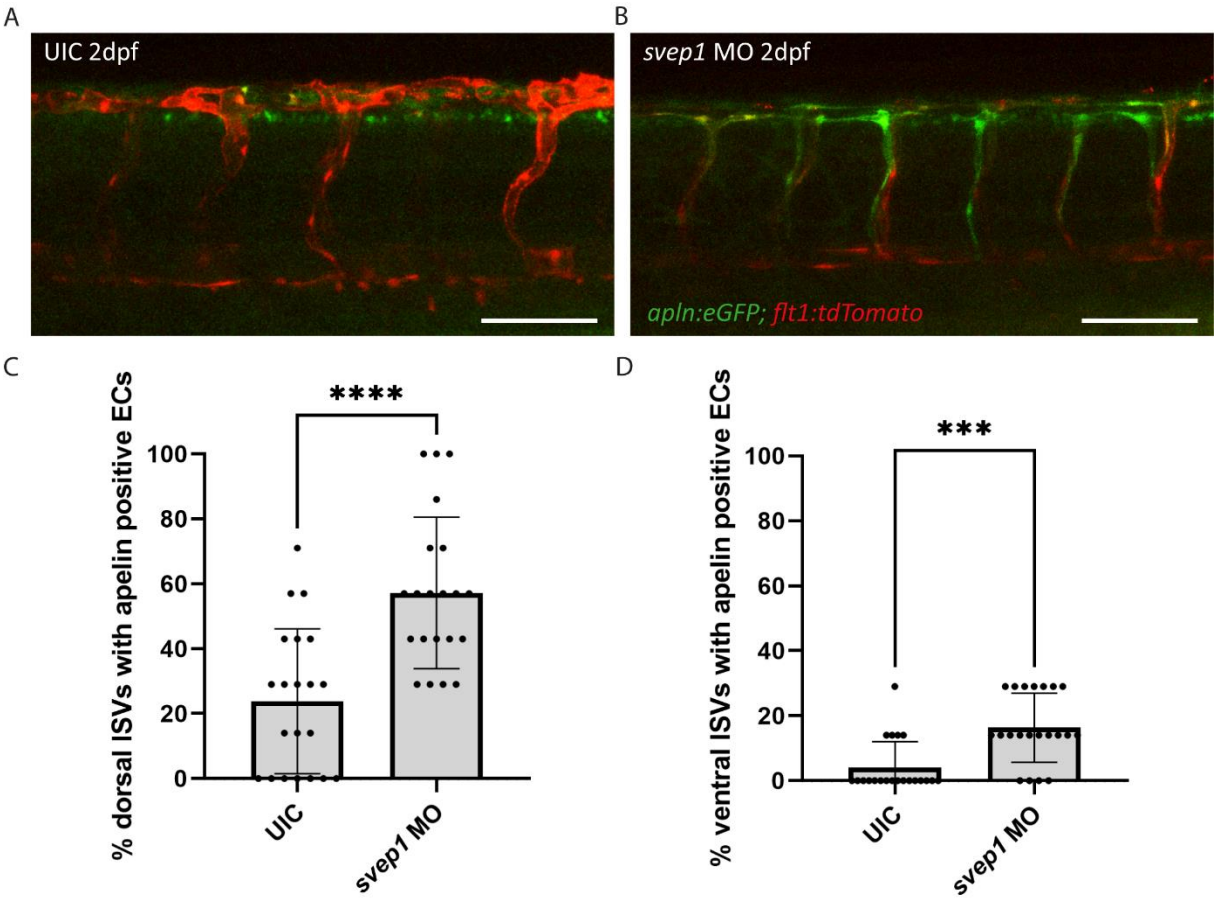

Supplementary figure 6: *svep1* morphants show increased apelin expression in ISVs

A) *apelin:eGFP* and *flt1:tdTomato* expression at 2 dpf in UIC compared to B) *svep1* morphants. C, D) Quantification of ISVs with apelin expression in dorsal and ventral parts of the ISVs. Dorsal part was counted from DLAV until midline region. Lateral region was counted from midline region onwards in ventral direction. *svep1* morphants showed significant increase of apelin positive ECs compared to siblings (UIC: n= 21; *svep1* MO: n= 21). Mann–Whitney test was applied for statistical analysis. Values are presented as means ± SD. ****P<0.0001, ***P=0.0002. Scale bar= 100 µm. UIC, uninjected control; hpf, hours post-fertilisation; ISV, intersegmental vessel.

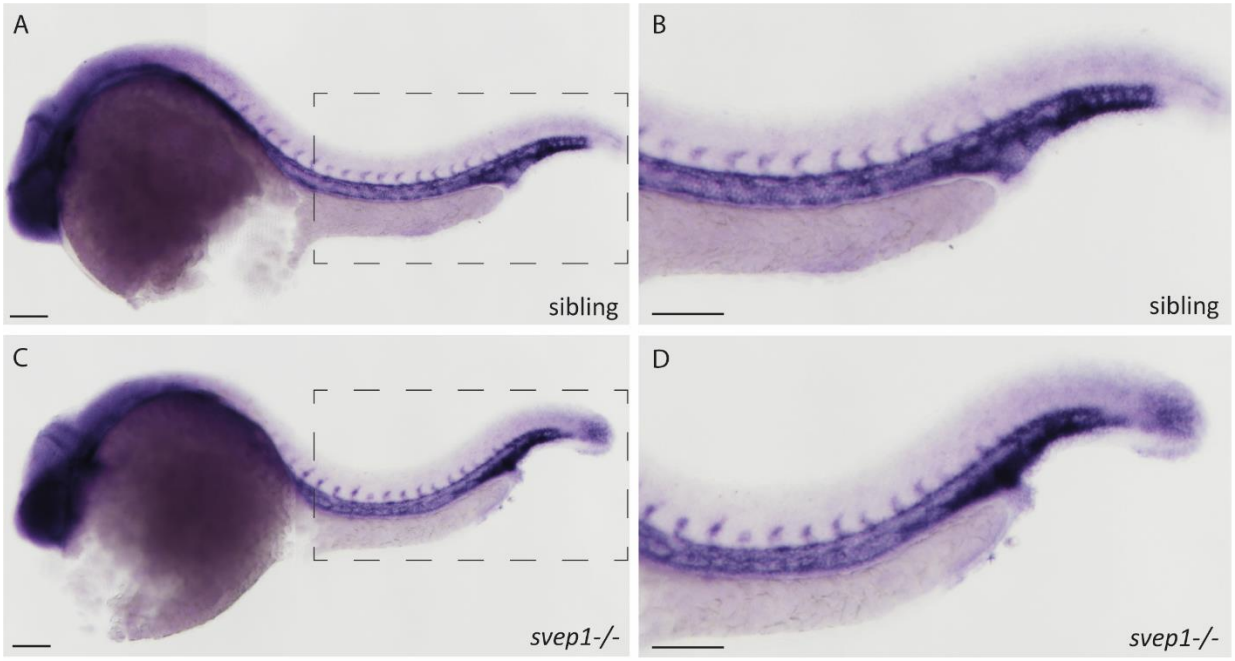

Supplementary figure 7: *tie1* expression is not altered in *svep1* mutants

In situ hybridization of *tie1* in *svep1* mutants (n=6) (C, D) and siblings (n=14) (A,B) at 24 hpf. Note that the images have been assembled from individual pictures to ensure proper focus of all areas. B and D are magnifications of boxed area in A and C respectively. Scale bar= 100µm.

gene	**wildtype 5'-3'**	**mutant 5'-3'**	common 5'-3'
adamts3 ^{hu10891}	GAAGGTGACCAAGTTCATGCTGCCATGGTGGAATGGCACGATG	GAAGGTCGGAGTCAACGGATTGCCATGGTGGAATGGCACGATC	TTCTGTTATCAGTCGCATTTCCAGC (reverse)
adamts14 ^{hu11304}	GAAGGTGACCAAGTTCATGCTTGGGAACAAACATCAACATTGTGCT	GAAGGTCGGAGTCAACGGATTTGGGAACAAACATCAACATTGTGCC	GCCTTACCTGTCGATATCCCACCA (reverse)
svep1 ^{hu6123}	GAAGGTGACCAAGTTCATGCTCCTGGTAGCACAGATATATCAGACTGT	GAAGGTCGGAGTCAACGGATTCCTGGTAGCACAGATATATCAGACTGA	GTTGTTGTGTGGTCTGTAGCCTTCC (reverse)
svep1 ^{hu4767}	GAAGGTGACCAAGTTCATGCTGGGGAGATGATGTCTCTTGCA	GAAGGTCGGAGTCAACGGATTGGGGAGATGATGTCTCTTGCT	CAGGCACTGTGCAGGTAAAGTCATT (reverse)
vegfc ^{hu6410}	GAAGGTGACCAAGTTCATGCTGGCTGCTTTCATCAATCTTGAACTTTT	GAAGGTCGGAGTCAACGGATTGGCTGCTTTCATCAATCTTGAACTTTA	GGCGGTTCTAAATTAATAGTCACTCACTT
tie2 ^{hu1667}	GAAGGTGACCAAGTTCATGCTGTCTTCTTGACGTACACCTCCTG	GAAGGTCGGAGTCAACGGATTGTCTTCTTGACGTACACCTCCTA	AGACTTCGGGCTGTCCAGAGGT
gene	**foward 5'-3'**	**reverse 5'-3'**	
ccbe1 ^{hu10965}	GCGCTGAACTTCAAGACTGG	ACAGACAGACAGCACAGCA	
tie1 ^{bns208}	TATTCCCACCACTCAGCAAG	ATGGTCACACAAGTCACAGC	
***tie1* primer for insitu probe generation**			
tie1 ISH probe 1	GGAGGAATGGTGCCTTTGGA	cattaaccctcactaaagggaaACATTGCCAAGCTGGTCTGA	
tie1 ISH probe 2	CGCTGAAGAGGCCTGACTAC	cattaaccctcactaaagggaaCTTGCGTTTTCTGGGCCAC	
tie1 ISH probe 3	TCATCCTCTACGCCTCTTCCT	cattaaccctcactaaagggaaGAGAGGTTAACGAGGAATAAAATGCA	

Supplementary table 1: primer list

References:

Alders, M., Hogan, B.M., Gjini, E., Salehi, F., Al-Gazali, L., Hennekam, E.A., Holmberg, E.E., Mannens, M.M., Mulder, M.F., Offerhaus, G.J., *et al.* (2009). Mutations in CCBE1 cause generalized lymph vessel dysplasia in humans. Nature genetics *41*, 1272-1274.

Aleström, P., D'Angelo, L., Midtlyng, P.J., Schorderet, D.F., Schulte-Merker, S., Sohm, F., and Warner, S. (2020). Zebrafish: Housing and husbandry recommendations. Laboratory animals *54*, 213-224.

Asakawa, K., Suster, M.L., Mizusawa, K., Nagayoshi, S., Kotani, T., Urasaki, A., Kishimoto, Y., Hibi, M., and Kawakami, K. (2008). Genetic dissection of neural circuits by Tol2 transposon-mediated Gal4 gene and enhancer trapping in zebrafish. Proc Natl Acad Sci U S A *105*, 1255-1260.

Astin, J.W., Haggerty, M.J., Okuda, K.S., Le Guen, L., Misa, J.P., Tromp, A., Hogan, B.M., Crosier, K.E., and Crosier, P.S. (2014). Vegfd can compensate for loss of Vegfc in zebrafish facial lymphatic sprouting. Development *141*, 2680-2690.

Bernier-Latmani, J., and Petrova, T.V. (2017). All TIEd up: mechanisms of Schlemm's canal maintenance. The Journal of clinical investigation *127*, 3594-3597.

Bos, F.L., Caunt, M., Peterson-Maduro, J., Planas-Paz, L., Kowalski, J., Karpanen, T., van Impel, A., Tong, R., Ernst, J.A., Korving, J.*, et al.* (2011). CCBE1 is essential for mammalian lymphatic vascular development and enhances the lymphangiogenic effect of vascular endothelial growth factor-C in vivo. Circulation research *109*, 486-491.

Bower, N.I., Koltowska, K., Pichol-Thievend, C., Virshup, I., Paterson, S., Lagendijk, A.K., Wang, W., Lindsey, B.W., Bent, S.J., Baek, S.*, et al.* (2017). Mural lymphatic endothelial cells regulate meningeal angiogenesis in the zebrafish. Nature neuroscience *20*, 774-783.

Bussmann, J., and Schulte-Merker, S. (2011). Rapid BAC selection for tol2-mediated transgenesis in zebrafish. Development *138*, 4327-4332.

Carlantoni, C., Allanki, S., Kontarakis, Z., Rossi, A., Piesker, J., Günther, S., and Stainier, D.Y.R. (2021). Tie1 regulates zebrafish cardiac morphogenesis through Tolloid-like 1 expression. Developmental biology *469*, 54-67.

Coxam, B., Collins, R.T., Hußmann, M., Huisman, Y., Meier, K., Jung, S., Bartels-Klein, E., Szymborska, A., Finotto, L., Helker, C.S.M.*, et al.* (2022). Svep1 stabilises developmental vascular anastomosis in reduced flow conditions. Development *149*.

D'Amico, G., Korhonen, E.A., Waltari, M., Saharinen, P., Laakkonen, P., and Alitalo, K. (2010). Loss of endothelial Tie1 receptor impairs lymphatic vessel development-brief report. Arteriosclerosis, thrombosis, and vascular biology *30*, 207-209.

Davis, S., Aldrich, T.H., Jones, P.F., Acheson, A., Compton, D.L., Jain, V., Ryan, T.E., Bruno, J., Radziejewski, C., Maisonpierre, P.C.*, et al.* (1996). Isolation of angiopoietin-1, a ligand for the TIE2 receptor, by secretion-trap expression cloning. Cell *87*, 1161-1169.

dos Reis, M., Thawornwattana, Y., Angelis, K., Telford, M.J., Donoghue, P.C., and Yang, Z. (2015). Uncertainty in the Timing of Origin of Animals and the Limits of Precision in Molecular Timescales. Current biology : CB *25*, 2939-2950.

Dumont, D.J., Gradwohl, G., Fong, G.H., Puri, M.C., Gertsenstein, M., Auerbach, A., and Breitman, M.L. (1994). Dominant-negative and targeted null mutations in the endothelial receptor tyrosine kinase, tek, reveal a critical role in vasculogenesis of the embryo. Genes & development *8*, 1897-1909.

Dumont, D.J., Gradwohl, G.J., Fong, G.H., Auerbach, R., and Breitman, M.L. (1993). The endothelial-specific receptor tyrosine kinase, tek, is a member of a new subfamily of receptors. Oncogene *8*, 1293-1301.

Eng, T.C., Chen, W., Okuda, K.S., Misa, J.P., Padberg, Y., Crosier, K.E., Crosier, P.S., Hall, C.J., Schulte-Merker, S., Hogan, B.M.*, et al.* (2019). Zebrafish facial lymphatics develop through sequential addition of venous and non-venous progenitors. EMBO reports *20*.

Gjini, E., Hekking, L.H., Küchler, A., Saharinen, P., Wienholds, E., Post, J.A., Alitalo, K., and Schulte-Merker, S. (2011). Zebrafish Tie-2 shares a redundant role with Tie-1 in heart development and regulates vessel integrity. Disease models & mechanisms *4*, 57-66.

Gordon, K., Schulte, D., Brice, G., Simpson, M.A., Roukens, M.G., van Impel, A., Connell, F., Kalidas, K., Jeffery, S., Mortimer, P.S.*, et al.* (2013). Mutation in vascular endothelial growth factor-C, a ligand for vascular endothelial growth factor receptor-3, is associated with autosomal dominant milroy-like primary lymphedema. Circulation research *112*, 956-960.

Hansen, T.M., Singh, H., Tahir, T.A., and Brindle, N.P. (2010). Effects of angiopoietins-1 and -2 on the receptor tyrosine kinase Tie2 are differentially regulated at the endothelial cell surface. Cellular signalling *22*, 527-532.

Helker, C.S., Eberlein, J., Wilhelm, K., Sugino, T., Malchow, J., Schuermann, A., Baumeister, S., Kwon, H.B., Maischein, H.M., Potente, M.*, et al.* (2020). Apelin signaling drives vascular endothelial cells toward a pro-angiogenic state. eLife *9*.

Helker, C.S., Schuermann, A., Karpanen, T., Zeuschner, D., Belting, H.G., Affolter, M., Schulte-Merker, S., and Herzog, W. (2013). The zebrafish common cardinal veins develop by a novel mechanism: lumen ensheathment. Development *140*, 2776-2786.

Hogan, B.M., Bos, F.L., Bussmann, J., Witte, M., Chi, N.C., Duckers, H.J., and Schulte-Merker, S. (2009). Ccbe1 is required for embryonic lymphangiogenesis and venous sprouting. Nature genetics *41*, 396-398.

Hogan, B.M., and Schulte-Merker, S. (2017). How to Plumb a Pisces: Understanding Vascular Development and Disease Using Zebrafish Embryos. Developmental cell *42*, 567-583.

Jeltsch, M., Jha, S.K., Tvorogov, D., Anisimov, A., Leppänen, V.M., Holopainen, T., Kivelä, R., Ortega, S., Kärpanen, T., and Alitalo, K. (2014). CCBE1 enhances lymphangiogenesis via A disintegrin and metalloprotease with thrombospondin motifs-3-mediated vascular endothelial growth factor-C activation. Circulation *129*, 1962-1971.

Jiang, Z., Carlantoni, C., Allanki, S., Ebersberger, I., and Stainier, D.Y.R. (2020). Tek (Tie2) is not required for cardiovascular development in zebrafish. Development *147*.

Joukov, V., Sorsa, T., Kumar, V., Jeltsch, M., Claesson-Welsh, L., Cao, Y., Saksela, O., Kalkkinen, N., and Alitalo, K. (1997). Proteolytic processing regulates receptor specificity and activity of VEGF-C. The EMBO journal *16*, 3898-3911.

Karkkainen, M.J., Haiko, P., Sainio, K., Partanen, J., Taipale, J., Petrova, T.V., Jeltsch, M., Jackson, D.G., Talikka, M., Rauvala, H.*, et al.* (2004). Vascular endothelial growth factor C is required for sprouting of the first lymphatic vessels from embryonic veins. Nature immunology *5*, 74-80.

Karlsson, J., von Hofsten, J., and Olsson, P.E. (2001). Generating transparent zebrafish: a refined method to improve detection of gene expression during embryonic development. Marine biotechnology (New York, NY) *3*, 522-527.

Karpanen, T., Padberg, Y., van de Pavert, S.A., Dierkes, C., Morooka, N., Peterson-Maduro, J., van de Hoek, G., Adrian, M., Mochizuki, N., Sekiguchi, K.*, et al.* (2017). An Evolutionarily Conserved Role for Polydom/Svep1 During Lymphatic Vessel Formation. Circulation research *120*, 1263-1275.

Kim, J., Park, D.Y., Bae, H., Park, D.Y., Kim, D., Lee, C.K., Song, S., Chung, T.Y., Lim, D.H., Kubota, Y.*, et al.* (2017). Impaired angiopoietin/Tie2 signaling compromises Schlemm's canal integrity and induces glaucoma. The Journal of clinical investigation *127*, 3877-3896.

Kizhatil, K., Ryan, M., Marchant, J.K., Henrich, S., and John, S.W. (2014). Schlemm's canal is a unique vessel with a combination of blood vascular and lymphatic phenotypes that forms by a novel developmental process. PLoS biology *12*, e1001912.

Kok, F.O., Shin, M., Ni, C.W., Gupta, A., Grosse, A.S., van Impel, A., Kirchmaier, B.C., Peterson-Maduro, J., Kourkoulis, G., Male, I.*, et al.* (2015). Reverse genetic screening reveals poor correlation between morpholino-induced and mutant phenotypes in zebrafish. Developmental cell *32*, 97-108.

Korhonen, E.A., Murtomäki, A., Jha, S.K., Anisimov, A., Pink, A., Zhang, Y., Stritt, S., Liaqat, I., Stanczuk, L., Alderfer, L.*, et al.* (2022). Lymphangiogenesis requires Ang2/Tie/PI3K signaling for VEGFR3 cell surface expression. The Journal of clinical investigation.

Le Guen, L., Karpanen, T., Schulte, D., Harris, N.C., Koltowska, K., Roukens, G., Bower, N.I., van Impel, A., Stacker, S.A., Achen, M.G.*, et al.* (2014). Ccbe1 regulates Vegfc-mediated induction of Vegfr3 signaling during embryonic lymphangiogenesis. Development *141*, 1239-1249.

Li, G., Nottebaum, A.F., Brigell, M., Navarro, I.D., Ipe, U., Mishra, S., Gomez-Caraballo, M., Schmitt, H., Soldo, B., Pakola, S.*, et al.* (2020). A Small Molecule Inhibitor of VE-PTP Activates Tie2 in Schlemm's Canal Increasing Outflow Facility and Reducing Intraocular Pressure. Investigative ophthalmology & visual science *61*, 12.

Maisonpierre, P.C., Suri, C., Jones, P.F., Bartunkova, S., Wiegand, S.J., Radziejewski, C., Compton, D., McClain, J., Aldrich, T.H., Papadopoulos, N.*, et al.* (1997). Angiopoietin-2, a natural antagonist for Tie2 that disrupts in vivo angiogenesis. Science (New York, NY) *277*, 55-60.

Mäkinen, T., Boon, L.M., Vikkula, M., and Alitalo, K. (2021). Lymphatic Malformations: Genetics, Mechanisms and Therapeutic Strategies. Circulation research *129*, 136-154.

Mäkinen, T., Norrmén, C., and Petrova, T.V. (2007). Molecular mechanisms of lymphatic vascular development. Cellular and molecular life sciences : CMLS *64*, 1915-1929.

Marron, M.B., Hughes, D.P., Edge, M.D., Forder, C.L., and Brindle, N.P. (2000). Evidence for heterotypic interaction between the receptor tyrosine kinases TIE-1 and TIE-2. The Journal of biological chemistry *275*, 39741-39746.

765 Martinez-Corral, I., Ulvmar, M.H., Stanczuk, L., Tatin, F., Kizhatil, K., John, S.W., Alitalo, K., Ortega, S.,
766 and Makinen, T. (2015). Nonvenous origin of dermal lymphatic vasculature. Circulation research *116*,
767 1649-1654.
768 Mauri, C., Wang, G., and Schulte-Merker, S. (2018). From fish embryos to human patients:
769 lymphangiogenesis in development and disease. Current opinion in immunology *53*, 167-172.
770 Michelini, S., Amato, B., Ricci, M., Serrani, R., Veselenyiova, D., Kenanoglu, S., Kurti, D., Dautaj, A.,
771 Baglivo, M., Compagna, R.*, et al.* (2021). SVEP1 is important for morphogenesis of lymphatic system:
772 Possible implications in lymphedema. Lymphology *54*, 12-22.
773 Morooka, N., Futaki, S., Sato-Nishiuchi, R., Nishino, M., Totani, Y., Shimono, C., Nakano, I., Nakajima,
774 H., Mochizuki, N., and Sekiguchi, K. (2017). Polydom Is an Extracellular Matrix Protein Involved in
775 Lymphatic Vessel Remodeling. Circulation research *120*, 1276-1288.
776 Okuda, K.S., Astin, J.W., Misa, J.P., Flores, M.V., Crosier, K.E., and Crosier, P.S. (2012). lyve1
777 expression reveals novel lymphatic vessels and new mechanisms for lymphatic vessel development in
778 zebrafish. Development *139*, 2381-2391.
779 Oliver, G., Kipnis, J., Randolph, G.J., and Harvey, N.L. (2020). The Lymphatic Vasculature in the 21(st)
780 Century: Novel Functional Roles in Homeostasis and Disease. Cell *182*, 270-296.
781 Padberg, Y., Schulte-Merker, S., and van Impel, A. (2017). The lymphatic vasculature revisited-new
782 developments in the zebrafish. Methods in cell biology *138*, 221-238.
783 Partanen, J., Armstrong, E., Mäkelä, T.P., Korhonen, J., Sandberg, M., Renkonen, R., Knuutila, S.,
784 Huebner, K., and Alitalo, K. (1992). A novel endothelial cell surface receptor tyrosine kinase with
785 extracellular epidermal growth factor homology domains. Molecular and cellular biology *12*, 1698-
786 1707.
787 Puri, M.C., Rossant, J., Alitalo, K., Bernstein, A., and Partanen, J. (1995). The receptor tyrosine kinase
788 TIE is required for integrity and survival of vascular endothelial cells. The EMBO journal *14*, 5884-
789 5891.
790 Roukens, M.G., Peterson-Maduro, J., Padberg, Y., Jeltsch, M., Leppänen, V.M., Bos, F.L., Alitalo, K.,
791 Schulte-Merker, S., and Schulte, D. (2015). Functional Dissection of the CCBE1 Protein: A Crucial
792 Requirement for the Collagen Repeat Domain. Circulation research *116*, 1660-1669.
793 Saharinen, P., Kerkelä, K., Ekman, N., Marron, M., Brindle, N., Lee, G.M., Augustin, H., Koh, G.Y., and
794 Alitalo, K. (2005). Multiple angiopoietin recombinant proteins activate the Tie1 receptor tyrosine
795 kinase and promote its interaction with Tie2. The Journal of cell biology *169*, 239-243.
796 Samarut, É., Lissouba, A., and Drapeau, P. (2016). A simplified method for identifying early CRISPR-
797 induced indels in zebrafish embryos using High Resolution Melting analysis. BMC genomics *17*, 547.
798 Sato, T.N., Tozawa, Y., Deutsch, U., Wolburg-Buchholz, K., Fujiwara, Y., Gendron-Maguire, M.,
799 Gridley, T., Wolburg, H., Risau, W., and Qin, Y. (1995). Distinct roles of the receptor tyrosine kinases
800 Tie-1 and Tie-2 in blood vessel formation. Nature *376*, 70-74.
801 Savant, S., La Porta, S., Budnik, A., Busch, K., Hu, J., Tisch, N., Korn, C., Valls, A.F., Benest, A.V.,
802 Terhardt, D.*, et al.* (2015). The Orphan Receptor Tie1 Controls Angiogenesis and Vascular Remodeling
803 by Differentially Regulating Tie2 in Tip and Stalk Cells. Cell reports *12*, 1761-1773.
804 Schindelin, J., Arganda-Carreras, I., Frise, E., Kaynig, V., Longair, M., Pietzsch, T., Preibisch, S., Rueden,
805 C., Saalfeld, S., Schmid, B.*, et al.* (2012). Fiji: an open-source platform for biological-image analysis.
806 Nature methods *9*, 676-682.
807 Schulte-Merker, S. (2002). Looking at embryos. In Zebrafish: a practical approach, C. Nusslein-
808 Volhard, ed. (New York, N.Y.: Oxford University Press), pp. p. 39–58.
809 Seegar, T.C., Eller, B., Tzvetkova-Robev, D., Kolev, M.V., Henderson, S.C., Nikolov, D.B., and Barton,
810 W.A. (2010). Tie1-Tie2 interactions mediate functional differences between angiopoietin ligands.
811 Molecular cell *37*, 643-655.
812 Shin, M., Nozaki, T., Idrizi, F., Isogai, S., Ogasawara, K., Ishida, K., Yuge, S., Roscoe, B., Wolfe, S.A.,
813 Fukuhara, S.*, et al.* (2019). Valves Are a Conserved Feature of the Zebrafish Lymphatic System.
814 Developmental cell *51*, 374-386.e375.

Suri, C., Jones, P.F., Patan, S., Bartunkova, S., Maisonpierre, P.C., Davis, S., Sato, T.N., and Yancopoulos, G.D. (1996). Requisite role of angiopoietin-1, a ligand for the TIE2 receptor, during embryonic angiogenesis. Cell *87*, 1171-1180.

Thévenaz, P., Ruttimann, U.E., and Unser, M. (1998). A pyramid approach to subpixel registration based on intensity. IEEE transactions on image processing : a publication of the IEEE Signal Processing Society *7*, 27-41.

Thomson, B.R., Heinen, S., Jeansson, M., Ghosh, A.K., Fatima, A., Sung, H.K., Onay, T., Chen, H., Yamaguchi, S., Economides, A.N.*, et al.* (2014). A lymphatic defect causes ocular hypertension and glaucoma in mice. The Journal of clinical investigation *124*, 4320-4324.

Thomson, B.R., Liu, P., Onay, T., Du, J., Tompson, S.W., Misener, S., Purohit, R.R., Young, T.L., Jin, J., and Quaggin, S.E. (2021). Cellular crosstalk regulates the aqueous humor outflow pathway and provides new targets for glaucoma therapies. Nature communications *12*, 6072.

Thomson, B.R., and Quaggin, S.E. (2018). Morphological Analysis of Schlemm's Canal in Mice. Methods in molecular biology (Clifton, NJ) *1846*, 153-160.

van Impel, A., and Schulte-Merker, S. (2014). A fisheye view on lymphangiogenesis. Advances in anatomy, embryology, and cell biology *214*, 153-165.

van Impel, A., Zhao, Z., Hermkens, D.M., Roukens, M.G., Fischer, J.C., Peterson-Maduro, J., Duckers, H., Ober, E.A., Ingham, P.W., and Schulte-Merker, S. (2014). Divergence of zebrafish and mouse lymphatic cell fate specification pathways. Development *141*, 1228-1238.

van Lessen, M., Shibata-Germanos, S., van Impel, A., Hawkins, T.A., Rihel, J., and Schulte-Merker, S. (2017). Intracellular uptake of macromolecules by brain lymphatic endothelial cells during zebrafish embryonic development. eLife *6*.

Venero Galanternik, M., Castranova, D., Gore, A.V., Blewett, N.H., Jung, H.M., Stratman, A.N., Kirby, M.R., Iben, J., Miller, M.F., Kawakami, K.*, et al.* (2017). A novel perivascular cell population in the zebrafish brain. eLife *6*.

Wang, G., Muhl, L., Padberg, Y., Dupont, L., Peterson-Maduro, J., Stehling, M., le Noble, F., Colige, A., Betsholtz, C., Schulte-Merker, S.*, et al.* (2020). Specific fibroblast subpopulations and neuronal structures provide local sources of Vegfc-processing components during zebrafish lymphangiogenesis. Nature communications *11*, 2724.

Young, T.L., Whisenhunt, K.N., Jin, J., LaMartina, S.M., Martin, S.M., Souma, T., Limviphuvadh, V., Suri, F., Souzeau, E., Zhang, X.*, et al.* (2020). SVEP1 as a Genetic Modifier of TEK-Related Primary Congenital Glaucoma. Investigative ophthalmology & visual science *61*, 6.